Volume 1 | Number 1 | Jan 2013 | Pages 1–100

Polymer Chemistry

www.rsc.org/polymers

ROYAL SOCIETY OF CHEMISTRY

This is an *Accepted Manuscript*, which has been through the Royal Society of Chemistry peer review process and has been accepted for publication.

Accepted Manuscripts are published online shortly after acceptance, before technical editing, formatting and proof reading. Using this free service, authors can make their results available to the community, in citable form, before we publish the edited article. We will replace this *Accepted Manuscript* with the edited and formatted *Advance Article* as soon as it is available.

You can find more information about *Accepted Manuscripts* in the Information for Authors.

Please note that technical editing may introduce minor changes to the text and/or graphics, which may alter content. The journal's standard Terms & Conditions and the Ethical guidelines still apply. In no event shall the Royal Society of Chemistry be held responsible for any errors or omissions in this *Accepted Manuscript* or any consequences arising from the use of any information it contains.

Polymer Chemistry

ARTICLE

Halogen Bonding in Polymer Science: From Crystal Engineering to Functional Supramolecular Polymers and Materials

Gilles Berger,[a] Jalal Soubhye[a] and Franck Meyer[b]

The halogen bonding (XB) is commonly defined as a non-covalent bond where halogen atoms (X = Cl, Br, I) function as electron acceptors. As an analogue of hydrogen bonding, halogen bonding is attracting a steady interest in many fields of research owing to the similarity of its concept. Thus, the combination of a high directionality and intrinsic hydrophobicity associated with a potential fine tuning of interaction strength makes XB a compelling tool for designing supramolecular functional materials. Over the last decade, an increasing number of instances was dedicated to the application of halogen bonding in polymer science by designing polymeric self-assembled components, organizing macromolecular entities and templating the formation of polymers. In this regard, the objective of this highlight will aim at emphasizing the recent developments of this approach by reviewing applications in topics as diverse as surface functionalization, soft, luminescent and magnetic materials, interpenetrated networks, synthetic methods, separation and inclusion techniques. The halogen bonds appear particularly tailored for engineering smart devices, and further applications in nanotechnologies through bottom-up approaches.

Introduction

Over the last two decades, supramolecular chemistry has become a major player in the design of highly functional materials.[1] On one hand, scientists elaborated a wide range of ever more sophisticated components, and on the other hand, the advent of non-covalent bonds allowed for an increase in complexity through self-organization.[2] Initially, the formation of supramolecular architectures was strongly inspired by Nature aiming at mimicking biological entities. However, the notion of molecular information permitted the implementation of complex systems and smart devices. To this end, chemist's imagination can rely on a prominent source of interactions. Biological entities and the abundant crystallographic database contain well-referenced non-covalent bonds, *i.e.* electrostatic forces, hydrogen bonding, $\pi - \pi$ and van der Waals interactions. It can be mentioned that other unusual weak forces such as cation$\cdots\pi$, anion$\cdots\pi$,[3] CH$\cdots\pi$ and lone pair$\cdots\pi$ contacts[4] endow a significant contribution in numerous supramolecular systems. Halogen bonding (XB) is in many aspects comparable to hydrogen bonding, being commonly defined as an interaction in which halogen instead of hydrogen atoms behave as acceptor of electronic density.[5] From the historical point of view, Guthrie first reported the formation of an interaction between a halogen

atom and an electron donor in 1863.[6] Then, a practical application of halogen atoms as recognition sites was mentioned by Hasselt in the 1960's.[7] At the end of the 1990's, Resnati developed the use of halogen bonding in the field of crystal engineering which was a significant turning point in XB-based solution and solid state supramolecular chemistry.[8,9,10] The main feature of XB lies in a positive region, or σ-hole, on the outermost surface of the halogen atom (X), along the extension of a C-X bond.[11,12] As a result, halogen bonding tends to be more directional than hydrogen bonding,[13,14] a negative electrostatic potential covering the equatorial region. In general, the strength of interaction follows the accepted trend I > Br > Cl. However, the presence of electron withdrawing groups linked to a halogen atom accounts for the strengthening of the σ-hole, allowing thus a fine tuning of XB interaction.[15] Over the last fifteen years, the self-assembly of modules by XB has thereby shifted from crystal engineering[16,17] toward the formation of functional materials.[18,19] It is worthy to note that the role of XB in biological systems has been recently highlighted,[20,21] and investigations are actually achieving increasing prominence since the halogen bond interaction tend to be less sensitive to polar or aqueous environments.[22,23,24,25]

Here, we decided to highlight the use of halogen bonding in polymer science. XB is still in its infancy and therefore only a few of instance is devoted to covalently bonded macromolecular structures. Compelling arguments convinced us to widen the scope of this review to non-covalently linked components which form 2 or 3 dimensional (2D or 3D) networks (supramolecular polymeric structures) with particular properties.[26] Indeed, the high strength and directionality of the halogen bonds are particularly suitable for designing highly functional materials, as it will be overviewed through different examples. This review does not pretend to be covering exhaustively the field of halogen bonded polymeric materials, but rather intends to bring a new approach/insight for the preparation of innovative materials. In this regard, different topics will be covered in this manuscript such as surface functionalization, soft, luminescent and magnetic materials, interpenetrated networks, and synthetic, separation and inclusion methodologies.

Surface functionalization

Flat substrates

Owing to the intrinsic properties of the fluorine atom, fluorination represents an appealing strategy to tune the physical and chemical features of active compounds.[27] Thus, fluorinated polymers are also of particular interest for coating and biomedical applications. In this respect, the formation supramolecular coatings was evaluated through the self-assembly of poly(4-vinylpyridine) (**P4VP**) and diiodoperfluoroalkanes thanks to N···I halogen bonds (**Figure 1**).
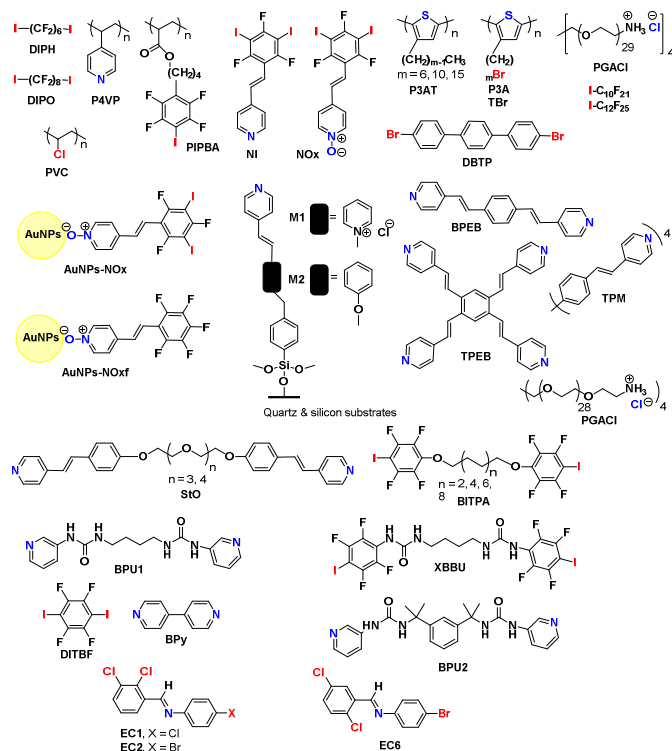
Figure 1. Structures of compounds involved in surface functionalization and soft materials

As proof of concept, 1,3-di(4-pyridyl)propane and ,6-diiodoperfluorohexane (**DIPH**) or 1,8-diiodoperfluorooctane (**DIPO**) formed supramolecular organizations governed by halogen bonding, as seen by X-ray diffraction analysis (**Figure 1**). Subsequently, **P4VP** was tested with 1,8-diiodoperfluorooctane in chloroform using 0.5:1 to 2:1 ratio of each compound, respectively. After evaporation of the solvent, FTIR absorption highlighted the presence of supramolecular N···I links by a blue-shift measured for pyridyl group absorption and a red-shift for C-I bond vibration by comparison with pure compounds. Further Thermal Gravimetric Analysis (TGA) of complex **P4VP**/diiodoperfluoroalkanes highlighted the presence of effective N···I interactions by a dramatic decrease of volatility of perfluorinated derivatives. Finally, the mesomorphic properties of system **P4VP(DIPH)**$_2$ were also determined by hot stage polarizing microscopy.[28]

Another approach has consisted in the fabrication of organic ultrathin films by layer-by-layer (LbL) assembly.[29] Taking into consideration the similarity between hydrogen and halogen bonds, Wang and co-workers evaluated the formation of polymeric multilayer film by N···I driving forces. Purposely, poly(4-(4-iodo-2,3,5,6-tetrafluorophenoxy)-butyl acrylate) (**PIPBA**) and complementary **P4VP** were synthesized and employed in film construction (**Figure 1**). The process was carried out by the successive immersion of NH$_2$-substrate in **PIPBA** and **P4VP** THF-chloroform solutions (1.9 x 10^{-3} mol (repeat units) L^{-1}), resulting in (**PIPBA/P4VP**)$_n$ multilayers. After having obtained characterization of LbL assembly by UV-vis absorption spectroscopy, halogen bonds were highlighted by X-ray Photoelectron Spectroscopy (XPS). By comparison with pure starting polymers, a clear shift in the binding energy of N 1s (BEN1s) and I 3d (BEI3d) (0.16 eV and 0.31 eV, respectively) accounted for the formation of a supramolecular complex between **PIPBA** and **P4VP**. X-ray reflection experiments and Atomic Force Microscopy (AFM) revealed a high coverage and a flat substrate, and the thickness of one bilayer was of about 1.3 ± 0.3 nm.[30]

Surface functionalization was also investigated by the growth of thin films on silicon substrates according to a Physical Vapor Deposition (PVD) technique. In this case, polymeric substances were elaborated through the self-assembly of self-complementary stilbazoles **NI** and **NOx** incorporating XB donor and acceptor functionalities (**Figure 1**). It is noteworthy that similar push-pull modules had demonstrated their ability to form supramolecular complexes with non-linear optic properties.[31,32] Single crystal structures of both compounds were consistent with the creation of networks supported by O···I and N···I halogen bonds in addition to NO···H-C contacts in **NOx**. Then, organic films were grown by PVD using a silicon and Cl$_3$Si(CH$_2$)$_{11}$CN-modified surfaces. As far as the film morphology is concerned, AFM images showed uniform grains regardless the surface for **NI**-based substrates. Conversely, the assembly of **NOx** gave rise to densely packed

Figure 1. Structures of compounds involved in surface functionalization and soft materials

grains on bare silicon (height = 30-60 nm) and uniformly distributed islands (height = 20-35 nm) on $Cl_3Si(CH_2)_{11}CN$-based surface. X-ray diffraction (XRD) of **NI** assemblies revealed a similar arrangement on both surfaces to that found in the single crystal lattice, in opposite to the organization of **NOx** on both substrates. The engineering of such materials could meet the requirement for the elaboration of optoelectronic devices.[33]

The relative organization of polymeric chains has a great impact on the performance of organic conjugated materials. Thus, the supramolecular arrangement of oligothiophenes has been achieved thanks to π-stacked aromatic and perfluoroaromatic rings due to opposite dipole moments.[34] Recently, the molecular self-assembly of regioregular poly(3-alkylthiophenes) has been investigated using XB as structure-directing agent. The synthesis of poly(3-alkylthiophenes) (**P3AT**) and poly(3-(ω-bromoalkyl)thiophenes) (**P3ATBr**) was done by Grignard's metathesis polymerization (GRIM), giving rise to polymers with a number average molecular weight (M_n) in the range 11 to 19.9 kg/mol (**Figure 1**). Subsequently, polymers deposited on highly oriented pyrolytic graphite (HOPG) were studied by Scanning Tunneling Microscopy (STM). Whereas well-organized 2D polycrystalline monolayers were determined for both compounds **P3AT** and **P3ATBr**, a drastic change of behaviour was observed after addition of a second layer. Surfaces composed of brominated **P3ATBr** displayed acute upper layers with parallel bundles which was in contrast with the random organization of poly(3-alkylthiophenes). The improved 3D organization found in **P3ATBr**-based substrates was thereby attributed to S···Br halogen bonds, providing an appealing strategy for generating 3D accurate conjugated materials.[35]

Another aspect of surface functionalization lies in the formation of porous supramolecular structures. Interesting applications can stem from these networks including catalysis, gas storage and sensing devices.[36] Here, the fabrication of 2D porous patterns relied on the self-assembly of 4,4''-dibromo-*p*-terphenyl (**DBTP**) on Ag(111) surface (**Figure 2**). The surface coating was performed at 150 K, designing three different square, rectangular and hexagonal motifs, as observed by STM. A particular feature of halogen atom lies in a positive σ-hole along the extension of a C-X bond but a negative electrostatic potential covers the equatorial region (**Figure 1**).
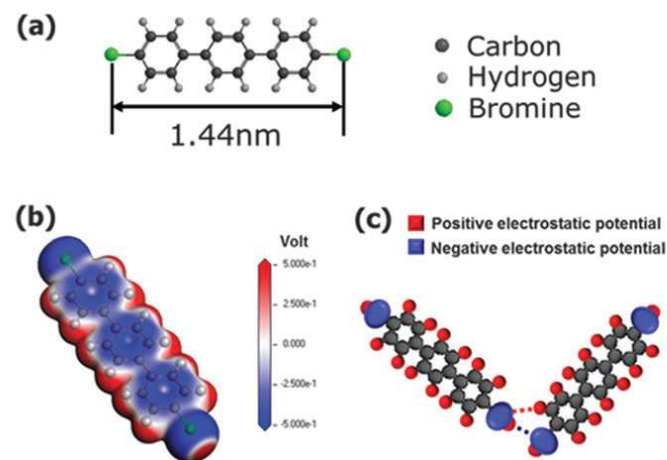
Figure 3. a) Chemical structure of the 4,4''-dibromo-*p*-terphenyl (**DBTP**) molecule. b) The calculated molecular electrostatic potential distribution of the **DBTP** molecule at the isodensity surface shown in red (positive) and blue (negative). c) Schematic for two **DBTP** molecules with simplified electrostatic potential distributions around H and Br atoms. Dotted lines indicate possible intermolecular bonds, Br···Br (blue) and H···Br (red). (Reproduced from Ref. [38] with permission from The Royal Society of Chemistry).

Therefore, bromide atom can act both as donor and acceptor of electronic density, as already seen with iodine atom.[37] As a consequence, self-assembled architectures were characterized by Br···Br and H···Br contacts with structural chirality in the case of square and rectangular patterns (Figure 3). As far as the geometry of networks is concerned, DFT calculations were in agreement with experimental results. Although hexagonal area (8.39 nm²) were larger than square (3.61 nm²) and rectangular (3.52 nm²) porous forms, calculated structures as function of lattice parameters revealed more favorable square and rectangular networks than hexagonal motif.[38]

Nanoparticles

Owing to their exceptional properties, carbon nanotubes (CNTs) have attracted a lot of interest for producing nanocomposite materials. In this regard, the dispersion of the CNTs in the polymer matrix can be performed by covalent or non-covalent functionalization, but the supramolecular approach is usually preferred due to the preservation of the π-conjugated surface of the nanofiller.[39] Hence, a large array of

Figure 2. (a)–(c) STM topography images of three porous networks obtained after a **DBTP** molecule was deposited on Ag(111) at 80 K. (d)–(f) High resolution STM images from the square marked areas of (a), (b), (c), respectively, which are superimposed with molecular models. Sizes of STM images: (a) 26 x 26 nm², (b) 26 x 26 nm², (c) 23.5 x 23.5 nm², and (d)–(f) 8 x 8 nm². For all images, tunneling current I_T = 0.1 nA and sample voltage V_S = 1 V (Reproduced from Ref. [38] with permission from The Royal Society of Chemistry).

non-covalent bonds has been employed for compatibilization such as π-π stacking and cation-π interactions but the halogen bonding remained underexplored.[40,41] With this in mind, nanocomposites were formed using poly(vinyl chloride) (**PVC**) with different tacticity and CNTs modified with ester functionalities (**Figure 1**). FTIR spectra of **PVC**/CNTs blends exhibited a variation of relative intensities in the region assigned to the C-Cl bond (550 and 750 cm⁻¹) by comparison with pure polymers. Interestingly, these variations increased with the content of isotactic sequences along the polymer backbone.[42] Thus, the better dispersion of the CNTs in the matrix was credited to specific C=O···Cl halogen bonds at the interface. Moreover, these non-covalent interactions provided a higher thermal stability and rigidity to **PVC**/CNT blends.[43,44]

In the arena of nanoparticles, gold species have attracted a steady interest as a result of their remarkable properties in fields of research as diverse as sensors,[45] microelectronics, catalysis,[46] imaging and biological treatments.[47] With the aim of determining the potential aggregation of gold nanoparticles (**AuNPs**) by XB, van der Boom and co-workers proposed to cover the **AuNPs** surface with aryl halides (**NOx**) and perfluorinated arene (**NOxf**) (not capable of XB), for the sake of comparison (**Figure 1**). Thus, the substitution of tetraoctylammonium bromide capping layer for **NOx** (or **NOxf**) provided new inorganic components where polar *N*-oxide entities function as coordination sites and XB donor groups point at the outer surface. As far as modified **AuNPs-NOx** and **AuNPs-NOxf** are concerned, Transmission Electron Microscopy (TEM) images highlighted individual nanoparticles arranged in chain-like structures but intermolecular interactions led to the formation of aggregates after 24h. The subsequent exposition of **AuNPs-NOx** to 1,4-bis((*E*)-2-(pyridin-4-yl)vinyl)benzene (**BPEB**) gave rise to supramolecular aggregates characterized by a change of color shifting from red to purple to blue, and by a shift of surface plasmon band. Moreover, an increasing **BPEB** concentration was found to affect the assemblies from chain-like to clustered structures due to halogen bonds. Unlike XB donor **AuNPs-NOx**, **AuNPs-NOxf/BPEB** did not show any variation of color or shift of surface plasmon band, as the consequence of the absence of interacting species.[48] Following the same principle, the same modified gold nanoparticles were used in the frame of a recognition process on self-assembled monolayers **M1** and **M2**. Purposely, quartz and silicon substrates were functionalized with (*E*)-1,2-di(pyridin-4-yl)ethane or (*E*)-4-(2-(pyridin-4-yl)vinyl)phenol where pyridyl groups point at the outer surface. The selective immobilization of **AuNPs-NOx** and **AuNPs-NOxf** has conducted to a high surface coverage on **M1** substrates whereas a coverage of **M2** surface of ~50% with **AuNPs-NOx** and <1% with **AuNPs-NOxf** was observed by Scanning Electron Microscopy (SEM). In this case, XB prevailed over the electrostatic interactions. In a second step, the film formation with modified **AuNPs** was carried out in the presence of ditopic and tetratopic connectors **BPEB**, **TPEB**, and **TPM**. After successive deposition steps, assemblies of **AuNPs-NOx** on monolayers developed halogen bonded

networks of densely packed and aggregated structures on **M1** and separate clusters on **M2**. Finally, the prevailing role of XB as driving force was emphasized by further deposition experiments on **M1** and **M2** substrates of **AuNPs-NOx** (without **BPEP**) or **AuNPs-NOxf** (with **BPEP**). In both cases, the stepwise assemblies resulted in the absence of additional absorption on the first mono-layer.[49]

In order to extend the field of surface functionalization, it can be mentioned that XB polymer brushes have not been investigated so far. In some cases, these polymeric systems exhibit stimuli responsiveness with a broad range of applications. The incorporation of XB donor groups along the polymer backbone should give rise to a new type of smart materials which is a topic investigated in our laboratory.[50,51,52,53]

Soft materials

Liquid crystals

Liquid crystalline materials consist in the self-organization of molecules into an anisotropic mode combining both the fluidity of a liquid and the anisotropy of a crystal.[54] First, we can make a brief overview of XB-based liquid crystals since this topic appears as one of the very first application of halogen bonding in materials science. Taking note of the analogy between hydrogen and halogen bonding, the deliberate design of XB-based mesomorphic materials was first reported in 2004[55] by the self-assembly of alkoxystilbazoles and iodopentafluorobenzene. Despite the non-mesomorphic nature of starting compounds, the supramolecular system showed liquid crystalline properties with a nematic to smectic A (SmA) behaviour. Then, investigations have turned their attention on the formation of trimeric supramolecular structures by the self-assembly through N···I interactions of stilbazoles with telechelic α,ω-diiodoperfluoroalkanes,[56] α,ω-bis(4-iodo-2,3,5,6-tetrafluorophenoxy) alkane derivatives[57] and 1,4-dihaloperfluoroarenes.[58] In all cases, the thermal behavior has revealed a predominant nematic and SmA mesomorphism. In 2010, a series of 90 dimeric couples supported by N···I halogen bonds were engineered in order to provide new insights on structure/mesomorphism relationships. The mesomorphic properties were able to be tuned from nematic to smectic as a function of the chain length of starting units and a chiral version provided chiral nematic and smectic A mesophases.[59] Afterwards, the combination of halogen and hydrogen bonding was also tested using 4-iodotetrafluorophenol and 4-alkoxystilbazoles. The three component systems were connected by N···I and N···H non-covalent bonds and the transition temperatures highlighted nematic and smectic A sequences.[60] Bent core liquid crystals are a very attractive class of mesomorphic materials which can develop chirality and polar order from achiral starting entities. Thus, ~~the~~ Bruce and co-workers studied the formation of V shaped structures using 1,3-diiodotetrafluorobenzene as halogen bond donor. The

resulting halogen bonded bent-core materials gave nematic to chiral nematic phase transitions despite the achiral character of starting units.[61] Finally, other unusual mesomorphic phases were obtained with trimeric halogen bonded structures, *i.e.* ordered calamitic phases (SmB and G) and a polar variation of SmA phase (SmAP).[62]

As far as supramolecular liquid crystalline polymers are concerned, the molecular structure of starting units has consisted in the design of telechelic α,ω-bis(4-iodo-2,3,5,6-tetrafluorophenoxy) alkane derivatives (**BITPA**) and stilbazole modules separate with oligoglycol linkers (**StO**) (**Figure 1**). In this respect, equimolar amounts of both complementary monomers in chloroform developed supramolecular polymeric structures, as confirmed by FTIR spectra. Then, the mesomorphic properties were investigated by polarizing optical microscopy (POM) and differential scanning calorimetry (DSC). It was observed a monotropic liquid crystallinity on cooling, the main feature of optical textures lying in droplet nematic phases. In this case, the presence of a flexible spacer between pyridyl rings appeared necessary since no mesomorphic phase transition was observed with rigid mesogens such as bipyridine derivatives.[63]

With the aim of organizing polymeric structures in a bottom-up fashion, supramolecular liquid crystals were formed due to a recognition process involving I⋯Cl⁻ interactions.[64] A semicrystalline 4-arm polyethylene glycol ~~flancked~~ end-capped with amine hydrochloride end groups (**PGACl**) was challenged with iodoperfluorodecane (**I-C$_{10}$F$_{21}$**) using a grinding procedure (**Figure 1**). First, FTIR experiments of **PGACl/I-C$_{10}$F$_{21}$** complex attested for a 1:1 optimized molar ratio of I/Cl⁻ interacting atoms. Then, DSC analyses supported by POM revealed a crystal-smectic A phase transition at 47 °C on heating. Further analyses determined the relative organization at the nanoscale. Small-angle X-ray scattering (SAXS) highlighted a highly ordered lamellar structure with an increased periodicity of 11.4 nm owing to the intercalation of fluorinated compound. In addition, SAXS reflection confirmed the stability of the supramolecular complex which was also found under mild conditions, *i.e.* upon heating and vacuum. The subsequent preparation of a **PGACl/ I-C$_{12}$F$_{25}$** complex by a vapor-phase insertion provided a new material with an overall alignment of constituents up to the millimeter scale thanks to halogen bonding and fluorophobic effects. It is interesting to note that the fluorinated compound can be removed under vacuum/thermal treatment.[65]

Gels

Another aspect of soft materials consists in supramolecular gels with switchable and controllable behaviors.[66,67] In the field of supramolecular low-molecular-weight gelators (LMWG), the urea α-tape hydrogen–bonding motif contributes to gel fibril formation, and the fine tuning of gel properties is possible under addition of anions or metal coordination owing to competing intermolecular interactions. With these data in mind, halogen bonding interaction was evaluated as turn on gelation by the self-assembly of bis(pyridyl urea) gelators **BPU1** and

PBU2 with 1,4-diiodotetrafluorobenzene (**DITFB**), and complex formation comprised of halogen bond donor bis(urea) **XBBU** with 4,4'-bipyridine (**BPy**), tetrabutylammonium iodide (**TBAI**) and **BPU1** (**Figure 1**). On fast cooling from 60 °C, an equimolar amount of **BPU1** and **DITFB** in a 4:1 methanol/water solution (1wt %) has arisen as optimized condition for hydrogel formation. The X-ray structure of **BPU1/DITFB** complex developed a two-dimensional sheet structure where α-tape hydrogen–bonding and N⋯I halogen bonding co-exist. In addition, Scanning electron microscopy (SEM) images of pure pro-gelator **BPU1** and the corresponding **BPU1/DITFB** system changed from 2D hexagonal plates to 1D needles, respectively (**Figure 4**). Following the same principle, the **BPU2/DITFB** system demonstrated the same gelation ability when equimolar quantities were mixed in a 5:4 methanol/water mixture.
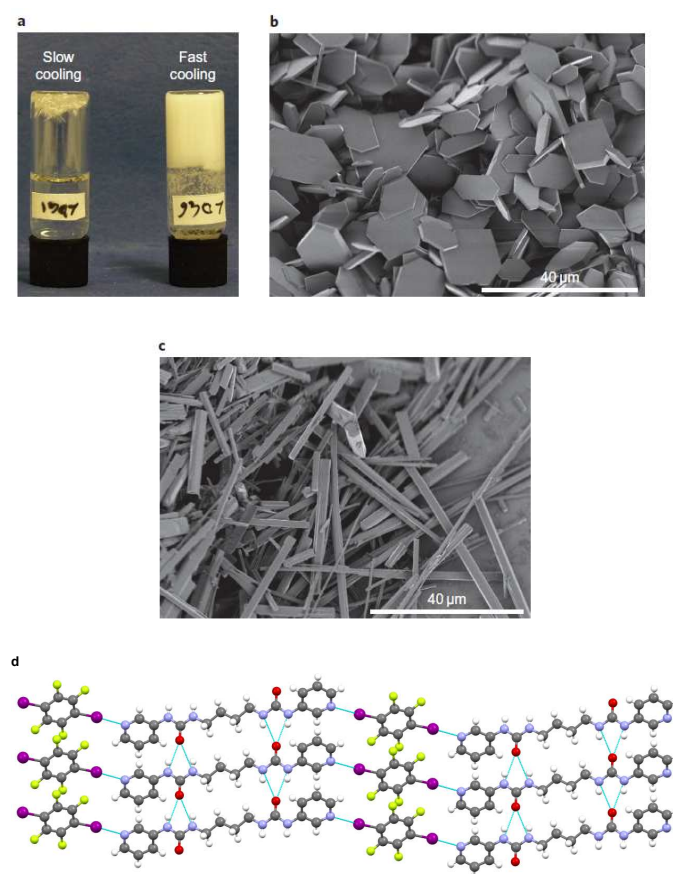
Figure 4. a) Rapid cooling of an equimolar mixture of bis(pyridyl urea) **BPU1** and **DITFB** in methanol/water (4:1 vol/vol) results in a robust hydrogel, while slow cooling gives a fibrous crystalline precipitate. b) SEM image of crystalline **BPU1**, which has a plate-like morphology. c) SEM image of **BPU1/DITFB**, which has a needle morphology. d) X-ray crystal structure of **BPU1/DITFB** showing the anticipated gel-forming urea–tape interaction and the halogen-bonding crosslinks involving the pyridyl groups. The crystalline materials in b–d were obtained under slow cooling conditions Colors are as follow: C, grey; H, white; O, red; N, blue; I, purple; F, yellow (Reproduced from Ref. [68] with permission from Nature Publishing Group).

Further X-ray diffraction of co-crystal **BPU2/DITFB** showed the presence of two water molecules hydrogen bonded to urea group and pyridyl ring, preventing thus the formation of urea α-tape organizations. Subsequently, the design of an expected single component gelator **XBBU** was realized by incorporation of bis(urea) and perfluoroaryliodide functionalities. Although **XBBU** did not exhibit any gelation properties, gels were obtained when **XBBU** was treated with **BPy** and **TBAI** in 3:1 DMSO/water mixtures (1wt %), but the **XBBU/TBAI** complex appeared unstable. In the same conditions, **XBBU** and **BPU1** were allowed to form a transparent brown gel upon cooling characterized by intricate homogeneous fibers, as seen by SEM.[68]

Elastic materials

Remarkable flexibility can be brought to crystalline organic materials by the interplay of a multitude of weak and dispersive interactions combined with corrugated packing. Following the preparation of elastic caffeine and 4-chloro-3-nitrobenzoic acid co-crystals by Ghosh and Reddy, halogenated N-benzylideneanilines showed to exhibit elasticity as organic crystals.[69]
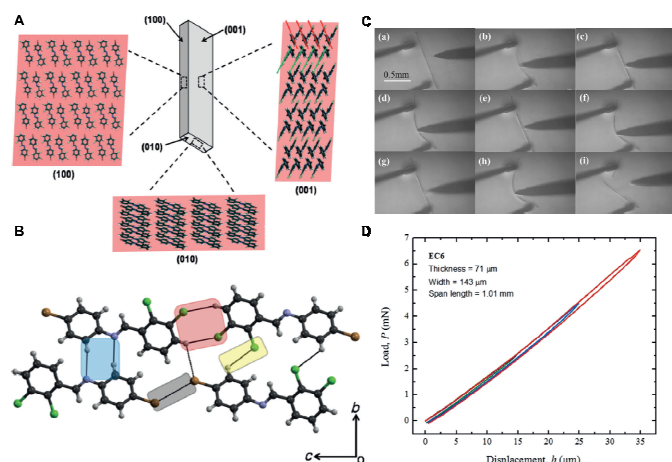
Figure 5. A. Crystal packing in EC2. Crystal morphology with face indices. Packing viewed down (001), (100), and (010) faces. Note that when the crystals are bent along [001], the (001) major faces are those that experience maximum tensile or contractile strains. In the major bendable face (001), red and green lines indicate a criss-cross arrange- ment (51° acute angle), which hinders long range of movement of molecules during bending. B. Hydrogen bond and halogen bond pattern with color code: C-H···N dimer (blue), C-H···Cl (yellow), C-H···Cl dimer (red), type I Br···Br (gray). C. Snapshots (a) through (h) of crystal EC1 to show bending cycles induced with a pair of forceps and a metallic needle. (i) The crystal breaks when it is bent beyond a threshold limit. D. Representative load-displacement (*P-h*) curves obtained (EC6) using the three-point bend test carried out using a nanoindenter, with increasing maximum displacements at the center of the span length. (Adapted from Ref. [69] with permissions from John Wiley and Sons).

Indeed, needle-shaped crystals built from seven halogenated N-benzylideneanilines revealed common characteristics and high flexibility. As a relevant example, 2,3-dichlorobenzylidine-4-bromoaniline (**EC2**) crystallized in the triclinic space group *P*1, showing interconnections through a multitude of weak

interactions: C-H···N, C-H···Cl and CH···Br hydrogen bonds, π···π stacking, and type I Br···Br halogen bond interactions (Figure 5**A** and **B**). These comparable yet moderate interactions along the three major directions gave rise to packing isotropy which, when combined with zig-zag packing that promotes interlocking of structural patterns, allowed an elastic behavior. The weak, dispersive interactions along the crystallographic planes act as "structural buffers" that can be readily broken or reformed, ensuring free molecular motion during bending. Halogen bonds seemed especially efficient in this regard, the large halogen atoms at the molecular peripheries providing good balance between directionality and the deformability needed to restore forces upon deformation.

The importance of XB in the elastic bending was highlighted by a comparison between **EC2** and **EC6** crystals, **EC6** involving a stronger Br···Cl (3.43 Å) halogen bond that the Br···Br (3.89 Å) of **EC2**. The strength of the halogen bond was reflected in the stiffness of the crystals, **EC6** giving rise to much stiffer crystals (bending stiffness of **EC2** and **EC6** are 91 and 179 Nm^{-1}, respectively). Criss-cross packing preventing long-range slipping was also essential for elasticity and lack of this feature led to plastic deformation.

Mukherjee and Desiraju also disclosed elastic bending of crystals made from 4-bromo-3- chlorophenol, which contrasted with the plastic deformation of 3,4-dichlorophenol. The authors rationalized this behavior by energetically comparable type II Br···Br interaction with the O-H···O hydrogen bond so that a degree of interaction isotropy was achieved.[70]

Aside from these considerations, this section is expected to be enriched in the near future with new halogen bonded components that can spontaneously repair. Indeed, self-healing materials are of particular significance to improve the lifetime, safety and reduce replacement costs.[71]

Luminescent and light responsive materials

Phosphorescent materials

Phosphorescent materials are commonly used in organic electronics, as well as chemical and biological sensing,[72] but purely organic molecules represent a very rare class of phosphors due to inefficient emission. The careful design of molecular structures targeting bright phosphorescence can consist of aromatic carbonyl compound for triplet generation and the presence of a heavy atom for singlet-triplet conversion. Under excitation at 360 nm, 2,5-dihexyloxy-4-bromobenzaldehyde (**Br6A**) was found weakly fluorescent in solution and a green phosphorescence was emitted at 500 nm in the solid state. The X-ray structure of **Br6A** highlighted strong C=O···Br halogen bonding, the O···Br distance being only 2.86 Å. Expecting a much more efficient emission under dilution, mixed crystals comprised of 2,5-dihexyloxy-1,4-dibromobenzene (**Br6**) and **Br6A** at ~0.001 wt% and ~1 wt% exhibited phosphorescent quantum yields of 55+3% and lifetimes of 8.3 ms. Structural modifications were subsequently

carried out giving rise to new crystals **BrC6A/BrC6**, **BrS6A/BrS6**, and **Np6A/Np6** with blue, yellow and orange phosphorescence, respectively (**Figure 9**).[73] Quantum yields were recently evaluated for mixed-crystals involving different chain lengths (2,5-dipentyloxy, 2,5-diheptyloxy, 2,5-dioctyloxy, respectively **Br5/BR5A**, **Br7/BR7A** and **Br8/BR8A**). Phosphorescence quantum yield always showed a maximum at 1 wt% loading of the emitter, the brighter mixed crystal being **Br6/BR6A**, yet **Br8/BR8A** gave almost similar results.[74] **Br6A** was also employed for the formation of amorphous phosphorescent polymeric materials. Purposely, a thin film with green phosphorescence was prepared using the bromine derivative (1 wt%) embedded in poly(methyl methacrylate) (**PMMA**) matrix. Interestingly, **Br6A**-based materials composed of isotactic **PMMA** showed higher quantum efficiency (7.5% quantum yield) than in atactic or syndiotactic polymers where halogen bonding affected positively the intersystem crossing. Further studies aimed at evaluating this system as temperature sensor using isotactic **PMMA**. In the range 30-60 °C, the phosphorescence intensity decreased upon heating and the emission intensity was determined reversible in consecutive cycles.[75] Following the same principle, a slight modification of **Br6A** alkyl chains into carboxylic acid functions provided a new organic phosphor denoted **G1**. AT room temperature, an aqueous solution of **G1** endowed a blue fluorescence at 460 nm with a quantum yield of 11.5% and a lifetime of 2.18 ns while at 77 K, the frozen system showed a strong green phosphorescence at 510 nm and a lifetime of 5.9 ms. The subsequent fabrication of drop casted films of poly(vinyl alcohol) (**PVA**) dopped with **G1** (1 wt%) gave rise to new phosphorescent materials. Hence, the resulting systems prepared with 80% and 100% hydrolyzed **PVA** displayed a phosphorescent emission with a quantum yield of 13% and 24%, respectively. Here, hydrogen and halogen bonds acted concomitantly: the hydrogen bonds suppressed the vibration/diffusion motion whereas intermolecular halogen bonds are responsible for spin-orbit coupling. Finally, the **G1-PVA** materials demonstrated a high sensitivity to humidity. Under addition of water, the system switched from green phosphorescence to blue fluorescence due to the disruption of hydrogen and halogen bonded networks. In such a way, these materials can find application in the development of water detection device.[76]

The formation of solid luminescent materials was also performed using 1,4-diiodotetrafluorobenzene (**DITBF**) and bent 3-ring-N-heterocycles, namely phenanthridine (**PHN**), benzo[ʃ]quinoline (**BfQ**) and benzo[h]quinoline (**BhQ**) (**Figure 9**). In **DITBF/PHN** complex (1:2 ratio), both units built a 2D supramolecular network comprised of cross-linked chains due to concomitant N···I and H···F contacts. As far as the **DITBF/BfQ** system is concerned, an equimolar amount of both modules gave rise to infinite zigzag chains through the combination of I···N, I···π, I···I halogen bonds and H···F hydrogen bonds. From the connectivity point of view, an original I···I···π pattern supported the supramolecular arrangement where an iodine atom acted both as halogen bond

donor and acceptor, the I···I and I···π distances being 3.7858(9) and 3.628(11) Å, respectively. Finally the crystallization from acetone of **DITBF** and **BhQ** in a 3:2 ratio gave a 2D supramolecular network where I···N, I···π, and H···I contacts co-exist. The phosphorescence properties of complexes **DITBF/PHN**, **DITBF/BfQ** and **DITBF/BhQ** moved from strong green to orange-yellow to orange, respectively, as the result of strong I···N and I···π halogen bonds (**Figure 6**).[77]

Figure 6. Photographs of phosphorescent co-crystals **DITBF/PHN**, **DITBF/BfQ** and **DITBF/BhQ** under 365 nm UV irradiation (Reproduced from Ref. [77] with permission from The Royal Society of Chemistry).

It can be mentioned that other works have reported the use of halogen bonds for inducing phosphorescence. A bromo-substituted capped γ-amino acid foldamer was crystallized from methanol and ethyl acetate solutions. The X-ray structure of resulting crystals exhibited C=O···Br halogen bondings responsible for a green phosphorescence under 254 nm UV light 78. The self-assembly of 1,4-diiodotetrafluorobenzene/N-methylcarbazole and 1,4-diiodotetrafluorobenzene/N-ethylcarbazole provided co-crystals emitting strong orange-red and weak pale yellow phosphorescences, respectively.[79]

Fluorescent materials

Following the same principle, fluorescent organic materials were elaborated from 1,4-bis-p-cyanostyrylbenzene (**BCSB**) which exhibit fluorescence properties, namely a yellow emission color. Thus, multi-color fluorescent materials were obtained through co-crystal formation in the presence of 1,4-diiodotetrafluorobenzene (**DITFB**), 1,4-diiodobenzene (**DIB**), 1,4-dibromotetrafluorobenzene (**DBTFB**) and 4-bromotetrafluorobenzene carboxylic acid (**BTFA**) (**Figure 9**). Complexes **BCSB/DITFB**, **BCSB/DBTFB** and **BCSB/BTFA** showed a blue-shift emission whereas co-crystal **BCSB/DIB** emitted a yellow/green color. X-ray structure afforded to highlight the structural organization of self-assembled systems. As expected, N···I halogen bonds governed the supramolecular arrangements of **BCSB/DITFB** and **BCSB/DIB**, resulting in the deaggregation of **BCSB**. As far as **BCSB/DBTFB** and **BCSB/BTFA** are concerned, 1D polymeric assemblies were developed due to N···Br interactions in addition to N···H hydrogen bonds in the case of **BCSB/BTFA**. Hence, the co-crystal formation in such a way offers a reliable strategy to tune the solid-state luminescent properties of a compound.[80] Additionally, the self-assembly of 5-iodo-isophthalic acid-containing coordination polymers was reported through I···I⁻ halogen bonds where a complex led to weak violet fluorescent emission bands under excitation.[81]

Light responsive materials

Another aspect of light responsive materials lies in azobenzene-based compounds capable of *trans-cis* isomerization under light exposure. Thus, photoresponsive polymers were designed by combining poly(4-vinylpyridine) (**P4VP**) and different dyes **DY** allowing either halogen or hydrogen interactions.[82, 83] First, **DY** species were co-crystallized with dipyridyl derivatives in order to model the **P4VP.DY** complexes. Trimeric systems were formed by the self-assembly of **DYI** or **DYOH** with 1,2-di(4-pyridyl)ethane and 1,3-di(4-pyridyl)propane as a result of N···I or N···H non-covalent bonds (**Figure 9**). In contrast, **DYBr** and **DYH** were not able to give supramolecular complexes under the same conditions. Subsequently, XPS analyses of spin cast thin films composed of (**P4VP.DY**)$_x$ (x = dye/polymer ratios) highlighted the supramolecular feature of the photoresponsive compounds by energy shifts for I 3d doublet in (**P4VP.DYI**)$_{0.2}$ and O 1s electron in (**P4VP.DYOH**)$_{0.2}$. After irradiation of (**P4VP.DY**)$_{0.1}$ samples (thickness ~ 90 nm), the first-order diffraction efficiency evolution was seen to increase as follows: **DYH < DYBr < DYOH < DYI** (**Figure 7**). Further experiments demonstrated that XB outperformed HB according to modulation depths of about 90 nm and 70 nm for (**P4VP.DYI**)$_{0.2}$ and (**P4VP.DYOH**)$_{0.2}$, respectively, and diffraction efficiencies in reflection mode of 5% and 4%, as well (**Figure 7**). Hence, the surface relief gratings efficiency appeared dependent of the nature of the non-covalent interaction between the photoactive chromophore and the polymer, *i.e.* the strength and directionality.[84]
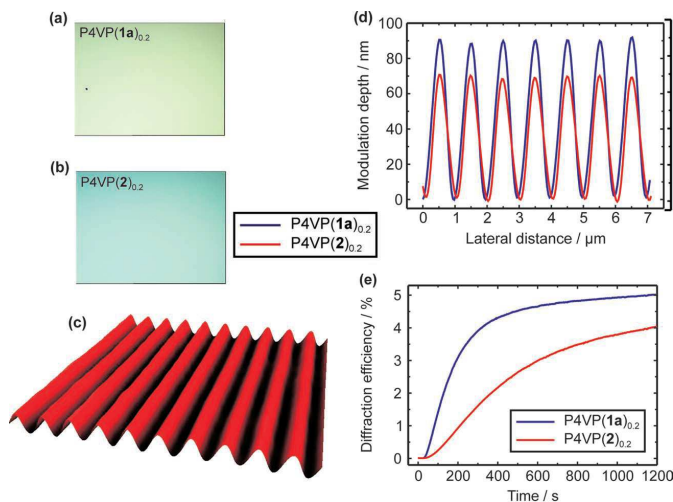
Figure 7. Characterization of spin-cast thin films of (**P4VP.DYI**)$_{0.2}$ and (**P4VP.DYOH**)$_{0.2}$ complexes. The sample thicknesses were ca. 110 nm and 100 nm for the films containing **DYI*** and **DYOH***, respectively. a,b) Optical microscopy images of thin films of (**P4VP.DYI**)$_{0.2}$ and (**P4VP.DYOH**)$_{0.2}$, respectively. c) Atomic force microscopy (AFM) surface profile of the SRG obtained from (**P4VP.DYI**)$_{0.2}$. d) The surface-modulation depths and e) the time evolution of the first-order diffraction efficiency of a He–Ne probe beam upon the SRG formation (Reproduced from Ref. [84] with permission from John Wiley and Sons).

* **DYI** = **1a** and **DYOH** = **2**

Following the same principle, the design of photoresponsive structures was investigated through the self-assembly of a halogen bond donor having an azobenzene group (**DYI**) and methoxystilbazole (**MeS**) (**Figure 9**). The short alkyl chain of non-mesogenic **MeS** appeared determinant to induce liquid crystallinity in the presence of **DYI** and to promote surface relief grating (SRG) formation. In this regard, the self-assembly of **DYI** and **MeS** was governed by N···I halogen bonding, the supramolecular complex exhibiting a monotropic nematic liquid crystalline phase on cooling. Subsequently, a spin-coated thin film (thickness ca. 250 nm) on glass substrate was irradiated with a 488 nm laser beam. The *trans-cis* photoisomerization of azobenzene derivative **DYI** induced a change of molecular packing. The film moved from crystalline to amorphous state, but the strong halogen bonds were still present in the irradiated isotropic film. When the crystalline film was irradiated with a linearly polarized light (488 nm) at room temperature, the randomly oriented molecules became align in the direction perpendicular to the polarization plane, with an order parameter of molecular alignment higher than 0.5. Finally, sample irradiation with a light interference pattern generated photoinduced SRG with surface-modulation depth of 600 nm, which was 2.4 times higher than the initial film thickness. The combination of the high directionality and controllable interaction strength makes the halogen bonds particularly suitable for designing photocontrollable suprastructures.[85] The same group performed a comprehensive study on surface patterning properties of an azobenzene library, confirming the superiority of XB versus HB in terms of SRG formation. The authors also introduced a new XB donor moiety, iodoacetylene (**DYIA**), which boosted surface patterns formation. DFT calculations showed that the iodoethynyl moiety beared halogen-bond donating properties comparable to that of perfluoroiodobenzene ones, however being potentially more directional. Co-crystals of **DYIA** with 1,2-di(4-pyridyl)ethylene resulted in short and linear halogen bonds with N···I distance of 2.754(3) Å and C–I···N angle of 175.29(10) °.
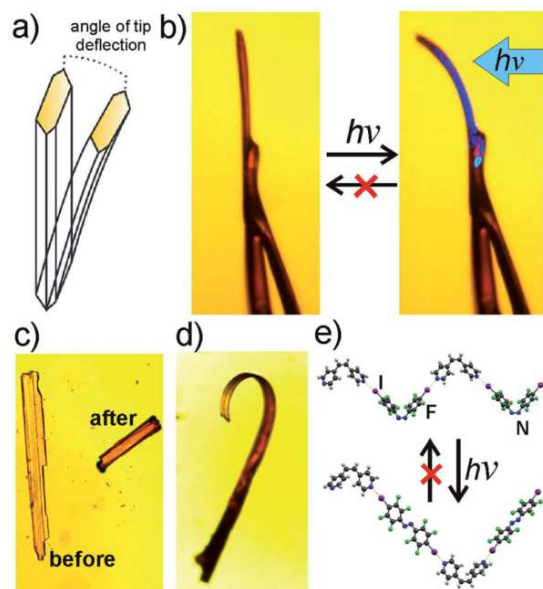
Figure 8. (a) Schematic illustration of the deflection of crystal tip upon photo-mechanical motion. (b) Permanent photo-mechanical change in shape of a (*cis*-**DYI₂**)(*cis*-**BPE**) cocrystal upon photochemical trans- formation into (*trans*-**DYI₂**)(*cis*-**BPE**), the blue arrow indicates the direc- tion of irradiation. (c) Comparison of a (*cis*-**DYI₂**)(cis-**BPE**) cocrystal before and after irradiation with 532 nm laser, the photochemical cis/trans isomerization is indicated by the color change of the irradiated co- crystal. (d) A highly bent crystal of (*cis*-**DYI₂**)(*cis*-**BPE**) with a tip deflection angle >90 °. (e) Fragments of cocrystal structures of the parent (top) and the daughter (bottom) phase involved in the photochemical transformation (*cis*-**DYI₂**)(*cis*-**BPE**) / (*trans*-**DYI₂**)(*cis*-**BPE**) (Reproduced from Ref. [86] with permission from The Royal Society of Chemistry).

When involved in supramolecular constructions with **P4VP**, it came as no surprise from this azobenzene library that XB strength following the order I > Br > F is reflected in SRG formation efficiency as well as in surface modulation depths. If diffraction efficiency and modulation depth are practically the same when comparing XB versus HB, the dynamics of the diffraction growth is significantly faster for halogen bonded supramolecular complexes, due to the higher directionality of XB over HB. Finally the iodoethynyl group brought a slight increase in SRG formation efficiency.[87] Remarkably, Bushuyev and coworkers were able to use light to shape crystals made of **DYI₂** and **DYBr₂**. Photomechanical shaping was achieved by irradiating single crystals of *cis*-azobenzene, so that photoisomerisation led to polycrystalline aggregate of their *trans*-isomers, in an irreversible manner. *Cis* to *trans* isomerization was made feasible by the long half-life of *cis*-**DYI₂**/**DYBr₂**, thus allowing their isolation as crystals. Irradiation (which is accompanied by a color change from yellow to orange) of the crystals allows bending in both directions owing to the irradiated face of the crystal. Metastable nature of *cis*-azobenzene together with the more efficient molecular packing (the volume of the unit cell per molecule decreasing from 339.5 Å^3 to 325.5 Å^3) of *trans*-azobenzene were the key parameters for this permanent bending.[88] They further demonstrated halogen bond-driven co-crystallization to be a simple strategy for generating a diversity of azo-based crystalline materials with different photo-mechanical and

thermal properties. Following the same approach as in [88], they reported a halogen-bonded *cis*-azo co-crystal (using *cis*- or *trans*-1,2-bis(4-pyridyl)ethylene and *trans*-4,4'-azopyridine as XB acceptors) that undergoes large-scale irreversible photo-mechanical bending in crystal-to-crystal fashion (**Figure 8**).
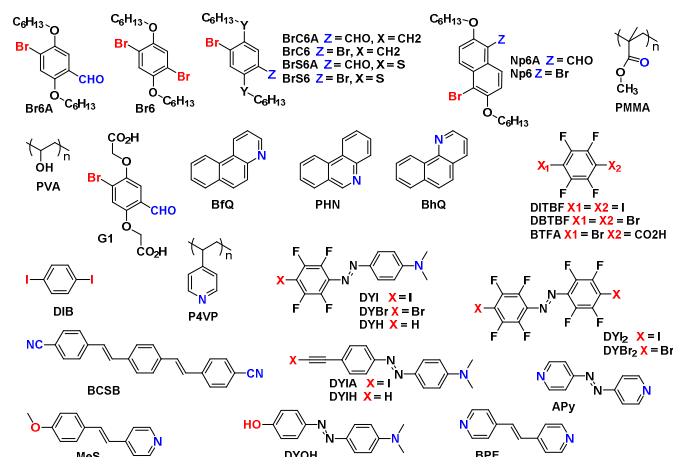
Figure 9. Structures of compounds involved in luminescent and light responsive materials

Interpenetrated networks

The design of interpenetrated architectures has always been an ambitious target in crystal engineering. Thus, the topological information of starting units can be translated to the supramolecular architecture, giving rise to entangled polymeric systems such as molecular catenanes and rotaxanes. These interpenetrating networks can endow a particular ability as the accommodation of a guest or the formation of porous materials.[89,90] In the last few years, Beer and coworkers have extensively investigated the recognition of anions using entangled systems. In 2010, the first rotaxane system based on the iodotriazolium group as XB donor exhibited a high selectivity toward the iodide anion.[91] Afterwards, rotaxanes incorporating a luminescent rhenium sensor were formed upon addition of anions. The interlocked host structure revealed to sense selectively halide anions over oxoanions, as monitored by luminescence spectroscopy.[92] Following the same principle, electrochemical measurements showed that a ferrocene-functionalized rotaxane can sense chloride anions.[93] Finally, a halogen bonded catenane was also obtained through the self-assembly of macrocycles possessing bromoimidazolium units and a bromide anion. This entangled structure bound selectively chloride and bromide anions.[94]

Neutral interpenetrated networks

In the frame of interpenetrated structures, tetrahedral modules are particularly attracting as their self-assembly can lead to diamondoid networks. The large open cavity of an adamantane-shaped motif is often prompted to interpenetration preventing thus the system of collapsing. With this in mind, the 4,4'-diiodo-4'',4'''-dinitrotetraphenylmethane (**DIDN**) was designed

with donor-acceptor self-complementary functionalities. After crystallization from nitromethane, the X-ray diffraction analysis of **DIDN** revealed the combination of 5-fold diamondoid and 3-fold square grid networks. The diamondoid net was characterized by I···O contacts of 3.379(13) Å whereas shorter I···O interactions (3.303(11) Å) supported the 2D grid net.[95] Following the same principle, neutral interpenetrated architectures were elaborated by means of halogen bond donor and acceptor tetrahedral units. Thus, tetradentate tectons were prepared by functionalization of pentaerythritol with pyridyl groups (tetrakis(4-pyridyl)pentaerythritol (**TKPE**)) and tetrafluoroiodobenzene groups (tetrakis(4-iodotetrafluoro-phenyl)pentaerythritol (**TKIE**)) (**Figure 12**). Subsequently, the co-crystallization of **TKPE** with **TKIE**, diiodoperfluoro-butane (**DIPB**), **DIPH** and **DIPO** was performed by the slow evaporation of ethanolic solutions of mixtures, followed by FTIR analysis of resulting crystalline materials. For all complexes, the ν_{C-H} absorption band of **TKPE** has shifted to higher frequencies with respect to pure **TKPE**, consistent with the electron donation from nitrogen to iodine. In opposite, the ν_{C-F} absorption band of fluorinated derivatives underwent a redshift by comparison with pure substances. The X-ray structures of these halogen bonded supramolecular complexes afforded to determine the mode of interpenetration with help of the TOPOS software.[96] The **TKPE/DIPH** system developed 2D square layers owing to N···I halogen bonds, the distances being in the range 2.72–2.75 Å. rom the topological point of view, the entangled structure is comprised of 2x2=4-fold interpenetration of class IIIa. As concerns the **TKPE/DIPH** units, the organization showed similar 2D square sheets (sql) thanks to N···I contacts with a degree of interpenetration of 5. In this case, the nodes are related by a simple translation, belonging thus to class Ia. Interestingly, the shorter diiodoperfluoroalkane **DIPB** provided a much complicated architecture. The complementary **TKPE/DIPB** modules have formed a 8-fold interpenetrated network of class Ia, the diamondoid cages (dia) being related by a single interpenetration vector. Finally, the self-assembly of **TKPE** and **TKIE** gave rise to a 10-fold diamondoid structure of class IIIa which is one of the highest degree of interpenetration for exclusive organic molecules reported to date (**Figure 10**). After careful analysis, this system appeared as 2x5=10 nets due to an interpenetration symmetry element.[97] In 2010, new entangled complexes were carried out using **TKPE** and tetrakis(4-pyridyl)cyclobutane (**TKCB**) as halogen bond acceptors. First, **TKPE** and 4,4'-diiodooctafluorostilbene (**DIFS**) were challenged in a 9:1 MeOH/CH$_2$Cl$_2$ solution which was allowed to evaporate at room temperature. The melting point of the solid residue (242-244 °C) has dramatically increased by comparison with starting materials (198 °C for **TKPE** and 207-210 °C for **DIFS**), which was in agreement with the formation of a supramolecular lattice. The X-ray structure was characterized by 2D square grids consisting of 3 interpenetrating nets of class Ia. The modules are held together due to N···I halogen bonds as defined by short N···I distances (~80% of the sum of Van der Waals radii of N and I) and almost linear N···I-C angles (175.3-

178.8°). A similar procedure led to the self-assembly of tetrakis(4-pyridyl)cyclobutane (**TKCB**) and **DITBF** (**Figure 10**). In this case, 2D square networks having a 4^4 topology were formed but the mode of interpenetration was of class IIa.[98]

Meanwhile, the use of a modified dendrimer was investigated in crystal engineering. Purposely, the poly(propylenimine) dendrimer DAB-*dendr*-(NH$_2$)$_2^2$ was decorated with tetrafluoroiodobenzene rings, giving rise to the DAB-*dendr*-(NH-C6F4I)$_2^2$ (**DAB1**) (**Figure 12**). The structural analysis featured intramolecular hydrogen bonds (four H···F and two H···N contacts) which locked the side chains in an extended conformation. Afterwards, DAB-*dendr*-(NH-C6F4I)$_2^2$ was challenged with *trans*-1,2-bis(4-pyridyl)ethylene (**BPy**) in a 1:2 ratio in a chloroform solution. Another time, good quality crystals were grown and characterized by a melting point (160-162 °C) definitely higher than that of starting materials (mp = 100-103 °C for **BPy**; mp = 148-152 °C for **DAB1**). The X-ray structure revealed the effective composition of the supramolecular system where a **DAB1** was linked to four **BPy** thanks to N···I halogen bonds. It can be mentioned that a π···π stacking between perfluoro- and pyridyl- rings also contributed to the stabilization of the framework. Thus, XB translated the topological information of the tetratopic unit to the entire architecture through the extended arms. From the geometrical point of view, 2D square networks with a 4^4 topology were formed, the side length of a rhombic unit reaching 34 Å. A careful analysis of the supramolecular lattice emphasized entangled square layers characterized by a 5-fold interpenetration of class Ia (**Figure 10**). In order to evaluate the sensing ability of such a compound, the 2nd and 3rd generation of modified dendrimers (DAB-*dendr*-(NH-C6F4I)$_2^3$ (**DAB2**) and DAB-*dendr*-(NH-C6F4I)$_2^4$ (**DAB3**)) were treated with a large excess of pyridine *N*-oxide in dichloromethane.[99] After repeated washing, the ^{1}H NMR spectra of resulting oily materials showed **DAB2**/ pyridine *N*-oxide and **DAB3**/ pyridine *N*-oxide ratio of 1.00:1.10 and 1.00:0.96, respectively.[100]

Ionic and coordination interpenetrated networks

The construction of halogen bonded architectures based on halide anions as electron donors has been extensively reported in the last ten years.[101] For instance, the selective recognition of anions by XB was carried out by the design of different types of receptors.[102,103] The Borromean rings constitute one of the most fascinating patterns of entanglement with a higher structural complexity. The peculiar topological feature possessed by Borromean links lies in their intrinsic mode of interpenetration. The three interlocked rings comprise an inseparable union, but remove any one and the other two form independent parts. In 1998, it was reported that 4,7,13,16,21,24-hexaoxa-1,10-diazabicyclo[8,8,8]-hexacosane (**K.2.2.2**) and diiodoperfluoroalkanes produced 1D polymeric chains by the interaction of nitrogen and iodine atoms.[104]
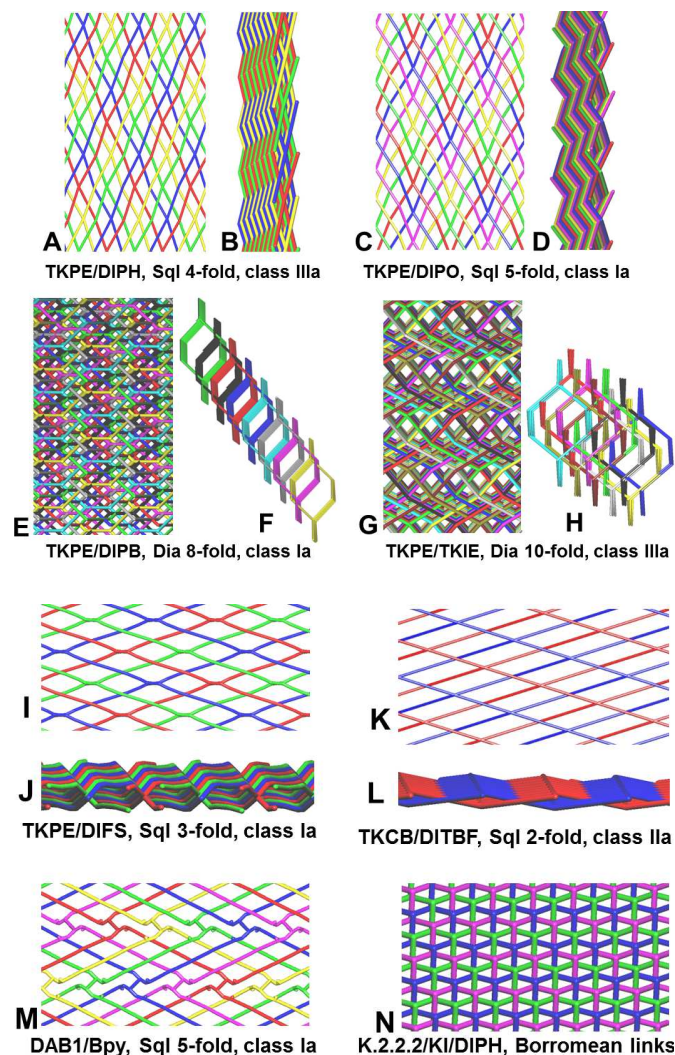
Figure 10. Schematic views obtained with TOPOS of interpenetrated networks **TKPE/DIPH** (A and B), **TKPE/DIPO** (C and D), **TKPE/DIPB** (E and F), **TKPE/TKIE** (G and H), **TKPE/DIFS** (I and J), **TKCB/DITBF** (K and L), **DAB1/BPy** (M) and **K.2.2.2/KI/DIPH** (N). (B), (D), (J) and (L): lateral views highlighting the mode of interpenetration. (F) and (H): isolated dia units showing the mode of interpenetration of class Ia and IIIa, respectively. (Image G reproduced from Ref. [97] with permission from Wiley, images I and K reproduced from Ref. [98] with permission from Elsevier, Image M Reproduced from Ref. [100] with permission from the American Chemical Society).

When a similar experiment was performed in the presence of potassium iodide (KI), the supramolecular structures showed a totally different organization. Indeed, the chelation of potassium cation by kryptant **K.2.2.2** set free an iodide anion particularly active as electron donor. When the self-assembly operated with **DIPH** and **DIPO** as electron acceptors, accurate 6.3 networks were defined by the iodide anions and perfluorocarbon (**DIPH** or **DIPO**) units (**Figure 12**). All iodide anions act as trivalent species toward three different perfluorinated modules which behaved, in turn, as telechelic halogen bond donors [105]. Both species developed a honeycomb-like structure with anions accommodated on the nodes of the hexagons and the perfluorocarbon forming the connectors. From the structural point of view, anions adopted a trigonal

geometry with a great precision, since the three I⋯I⁻ contacts and I⋯I⁻⋯I angles were identical in **K.2.2.2/KI/DIPH** (3.513 Å and 72.24°) and **K.2.2.2/KI/DIPO** (3.474 Å and 73.06°). The main feature of both systems lied in a characteristic undulating pattern with large cavities created by the long fluorinated spacers **DIPH** or **DIPO**. An entanglement of translationally related grids was elucidated by the examination of the polymeric complexes, consistent with a specific interpenetration into Borromean links (**Figure 10**). In addition, the thickness of fluorinated layers can be adjusted carefully by using the appropriate perfluorocarbon unit.[106]

Recently, investigations on coordination polymers have turned their attention on the construction of metal organic frameworks using the halogen bonds as structure directing agent.[107] Hence, entangled systems were constructed through self-assembly of zinc and cadmium ions, flexible ligands (**bmib**, **ditb** and **ditp**) and **H2tbtpa** (**Figure 12**). The presence of bromine atoms on the aromatic group was expected to supplement the coordinative interactions by secondary halogen bond interactions. In this regard, starting compounds were stirred in sealed tubes at 120 °C followed by the slow cooling to 30 °C which allowed the crystallization of resulting coordination complexes. According to the X-ray diffraction analysis of $[Zn_2(bmib)(tbtpa)_2 \cdot 2H_2O]_n$, a 4-fold interpenetrating network with a diamondoid topology was developed. From the topological point of view, the entangled system consisted in a 2x2=4-fold interpenetration of class IIIa according to the previous classification due to a symmetry element. The interpenetrated network was supported by connections between zinc (II) ions and **bmib** ligands. However, additional weak interactions were present in the structure, namely H⋯O hydrogen bonds between water and **tbtpa**, and two Br⋯Br halogen bonds of 3.563(3) and 3.557(3) Å. In the same crystallization conditions, complexes $[Cd(ditb)(tbtpa)(H2O)_2 \cdot 2H_2O]n$ and $[Zn(ditp)(tbtpa)]n$ gave rise to 2D polymeric layers with a 4^4 topology and (6.3) honeycomb motif, respectively. Another time, halogen bonds contributed to the stability of the supramolecular complexes. Hence, Br⋯O and Br⋯Br contacts were observed in both structures. On cooling at 77 K, a fluorescence emission of ~2.2 nanoseconds was measured for $[Cd(ditb)(tbtpa)(H_2O)_2 \cdot 2H_2O]n$ and $[Zn(ditp)(tbtpa)]n$.[108]

With the aim to accommodate conducting molecules in 2D or 3D networks, Fourmigué and co-workers designed the tridentate 1,3,5-tris(iodoethynyl)-2,4,6-trifluorobenzene (**TITF**) and undertook its co-crystallization with a variety of organic salts (**Figure 12**). The expected (6.3) honeycomb patterns formed by anion⋯I interactions were supposed to be filled by cations or interpenetrated networks. In this regard, a range of ammonium, phosphonium, sulfonium iodides and bromides and less common *N*-methyl-diazabicyclooctane iodide and bis(triphenylphosphoranylidene)ammonium chloride were evaluated. Focusing on the entangled systems, the 1:1 adducts composed of **TITF**/Bu3SI and **TITF**/Et3MeNI delivered (6.3) networks with 2-fold and 4-fold interpenetrations. Thus, the iodide anion in **TITF**/Bu3SI maintained its trivalent

coordination toward three different **TITF**. The resulting cavities were filled by another lattice which gave rise to a 2-fold halogen bonded interpenetrated network of class Ia. As far as **TITF**/Et3MeNI is concerned, a much more complicate structure was obtained comprising additional chloroform molecules. The iodide anion coordinated three iodine atoms of three **TITF** but a 3D halogen bonded architecture was generated. As concerns the topology, the 3D anionic network was characterized by a 4-fold interpenetration of class IIIa due to inversion and symmetry elements.[109]

Synthetic chemistry

In the field of catalysis, hydrogen bonding and transition metals represent powerful instruments in the chemist's toolbox. However, organocatalysis presents an environmental advantage over metal based catalysts for activation of electrophile towards a nucleophilic attack. Thus, the development of halogen bonded catalysts has slowly emerged in the panel of synthetic methodologies with a research work reported by Bolm in 2008. The reduction of 2-phenylquinoline using a Hantzsch ester was made possible through the assistance of haloperfluoroalkanes as catalysts. The iodo derivatives outperformed the bromoperfluoroalkanes since only 1 mol% of perfluorohexyliodide appeared sufficient for the formation of tetrahydroquinoline in 69% yield.[110] Very recently, the same transfer hydrogenation of quinolone, quinoline, pyridine and imine derivatives was carried out with a bidentate imidazolium XB donor. The reduction of C=N bonds with Hantzsch ester provided the corresponding adducts in an efficient way for quinolines and imines with a catalyst loading of only 2%.[111] Then, a Ritter-like reaction has consisted in the conversion of benzhydryl bromide into *N*-benzhydryl acetamide with 2-iodoimidazolium derivatives as activating agents. Reactions required an equimolar amount of catalyst to obtain the acetamide in 80 to 97% yields.[112,113] A similar reagent afforded the activation of carbonyl group in the frame of a Diels Alder reaction. By comparison with a thiourea catalyst, a 20 mol% of halogen bond donor was sufficient to yield the cycloadduct in 63% after 6h.[114] Very recently, 2-halogenoimidazolium catalyzed aza Diels-Alder reaction between N-phenylbenzaldimine and Danishefsky diene has been reported. Reaction proceeded with very good yields (up to 85%) within 1 hour at room temperature and in the presence of 5 mol% of the catalyst, whereas no reaction was observed without the catalyst or using weaker XB donors.[115]

[2+2] photocyclization reactions

The [2+2] photocyclization reaction in the solid state offers an original and useful alternative to the formation of covalent bonds in a regio- and stereoselective fashion. Thus, a photocycloaddition occurs when two double bonds meet the requirement postulated by Schmidt, namely a parallel orientation separated by a distance spanning from 3.5 to 4.2 Å.[116] With these data in mind, the tetratopic XB donor **TKIE** was exploited as template in order to organize *trans*-1,2-bis(4-

pyridyl)ethylene units (**BPy**) according to the specific geometric criteria (**Figure 12**). Pentaerythritol derivative **TKIE** was co-crystallized with **BPy** in a 1:2 ratio, giving rise to good crystals for X-ray diffraction experiment. As expected, modules have self-assembled into a 1D infinite ribbon governed by N⋯I connectivities. These interactions were characterized by typical parameters for halogen bonded complexes, *i.e.* a reduction of the N⋯I distances (~ 80% of the sum of the van der Waals radii) and almost linear N⋯I-C angles (~177°). In addition to XB, a π⋯π stacking occurred between the fluorinated aromatic groups of **TKIE** separated by a distance in the range 3.524-3.897 Å. As a result, the supramolecular polymeric arrangement was constituted of pre-organized olefinic modules with a parallel alignment of double bonds (separation lower than 4.5 Å), which fulfilled the topochemical postulate. Finally, the finely powdered material was irradiated at 300 nm for 3h, yielding stereospecifically and quantitatively the resultant *rctt*-tetrakis(4-pyridyl)cyclobutane (**TKCB**), as determined by NMR and GC analyses.[117]

This successful strategy was subsequently applied to the photo-dimerization of a self-complementary tecton. Purposely, a telechelic heteroditopic derivative **DMAS** was designed with *N,N*-dimethylaniline and iodotetrafluorobenzene end groups targeting a an efficient pre-organization into supramolecular polymeric structures. After crystallization from a chloroform solution, the crystal packing disclosed by X-ray diffraction revealed the formation of a wavy linear pattern supported by N⋯I contacts with a distance 12% shorter than the sum of van der Waals radii. Olefins were pre-organized in a head-to-tail fashion owing to a π⋯π stacking between aromatic rings of opposite quadrupolar moments. The optimal arrangement led to paired modules where the distance between the double bonds was only 3.758 Å, consistent with the topochemical criteria for a [2+2] photocyclization in the solid state. The crystalline material was subsequently irradiated at 300 nm for 24h, which afforded the conversion of **DMAS** into its corresponding cycloadduct **BICB** in 80% yield, as determined by ^{1}H NMR spectroscopy (**Figure 12**). The X-ray diffraction analysis of **BICB** attested for the *rctt* stereochemistry of the cyclobutane ring. In addition, the heterotetratopic self-complementary tecton formed a 2D infinite network due to new N⋯I halogen bonds (N⋯I distances of 2.907 Å) with clathrated chloroform molecules.[118]

Polymerization reactions

Another aspect of solid state synthesis consists in the topochemical 1,4-polymerization of diynes. Geometric constraints require the careful positioning of monomer diynes at a repeat distance of 4.9 Å and an orientation angle of 45° relative to the translation axis. Moreover, the 1,4-polymerization reaction necessitates the adjustment of the C1-C4 distance between successive monomer diynes at 3.5 Å. An early report of Lauher and Goroff described the 2D supramolecular organization of diynes owing to the combination of hydrogen and halogen bonding. 1D hydrogen bonded networks were achieved by the self-assembly of

oxalamide or urea hosts which induced a thin alignment of halogen bonded diyne guests according to the structural guideline.[119] However, slight variations with respect to the topochemical postulate prevent the polymerization. New host compounds (**OX1** to **OX3**) possessing oxalamide functions as primary directing structure were designed with nitrile end groups as weak halogen bond acceptor. Recognition processes of 1,4-diiodo-buta-1,3-diyne (**DBD**) and **OX** templates were operated in methanol in a 1:1 ratio but only **OX2** and **OX3** were allowed to form a supramolecular complex (**Figure 12**). The X-ray structure of **DBD/OX2** highlighted the perfect organization of diyne units thanks to the high directionality of XB supplemented by hydrogen bonded oxalamide networks. As far the polymerization is concerned, the attempt failed due to a repeat distance of 5.25 Å higher than the targeted 4.9 Å. Surprisingly, the structural analysis of system **DBD/OX3** is comprised of only the poly(diiododiacetylene) (**PIDA**) (**Figure 11**). During the crystallization process, the remarkable organization of diyne units entailed a spontaneous polymerization. The flexibility of oxalamide side chains and the weak XB interactions appeared as favorable parameters for the macromolecule preparation.[120]
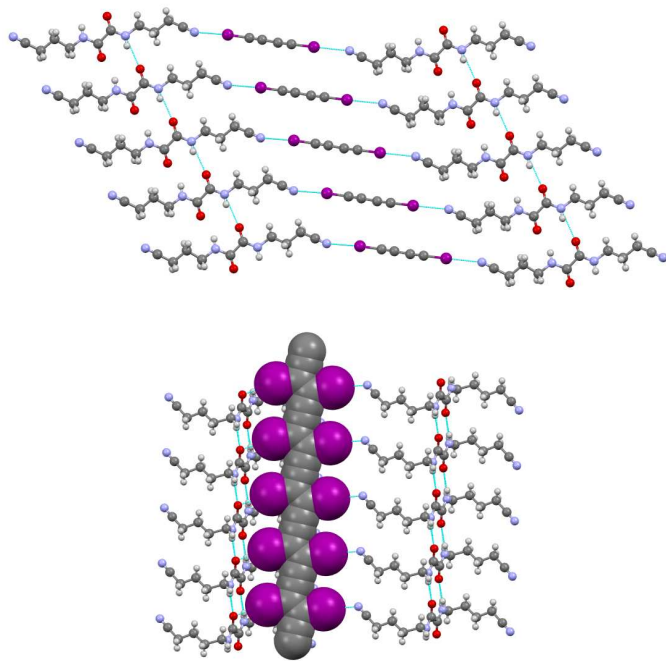
Figure 11. X-ray structure of **DBD/OX2** complex highlighting the perfect organization of diyne units (up). X-ray structure of **PIDA** (space-filling) and host **OX3** (down). Colors are as follow: C, grey; H, white; O, red; N, blue; I, purple.

In the field of the ring opening polymerization (ROP) of cyclic esters, tin octoate is probably the most often used catalyst.[121] However, investigations have slowly turned their attention towards new organocatalysts such as 1,8-diazabicyclo[5.4.0]undec-7-ene (DBU) or 1,5,7-triazabicyclo[4.4.0]dec-5-ene (TBD).[122] To this end, a simple halogen bonded catalyst (iodine trichloride (**ICl₃**)) was studied for the controlled ring opening polymerization of L-lactide

(**LA**) (Figure 12). Preliminary investigations aimed at determining the electrophilic activation of carbonyl groups. Under addition of **ICl₃** to a chloroform solution of **LA**, FTIR spectra highlighted a clear shift of the C=O vibrational signal (*ca*. 1759 to 1772 cm^{-1}), in agreement with the electron donation from the oxygen toward the iodine. Moreover, ^{13}C NMR spectroscopy measurements also evidenced a variation of chemical shift assigned to the carbonyl group (~ 1.8 ppm). As concerns the nucleophilic initiator of ROP, ^{1}H NMR spectra confirmed an additional activation of 11-bromo-1-undecanol (**BOH**) through OH⋯Cl hydrogen bonds. Subsequently, the ROP of **LA** was performed under classical conditions, *i.e.* at room temperature in chloroform. Hence, the polymerization kinetic appeared dependent of the initiator/catalyst ratio. An equimolar amount of **BOH/ICl₃** led to a conversion of only 35% after 71h (Mn = 2.5 kg/mol and a polydispersity index (PDI) = 1.3). In contrast, a **BOH/ICl₃** ratio 1:15 provided the poly(L-lactide) in 44h (conversion = 86%) with a molecular weight of 21.3 kg/mol and a PDI of 1.4, as determined by gel permeation chromatography. Further electrospray ionization mass spectrometry studies corroborated the controlled character of the polymerization through determination of poly(L-lactide) exclusively end-capped with **BOH** residues.[123]
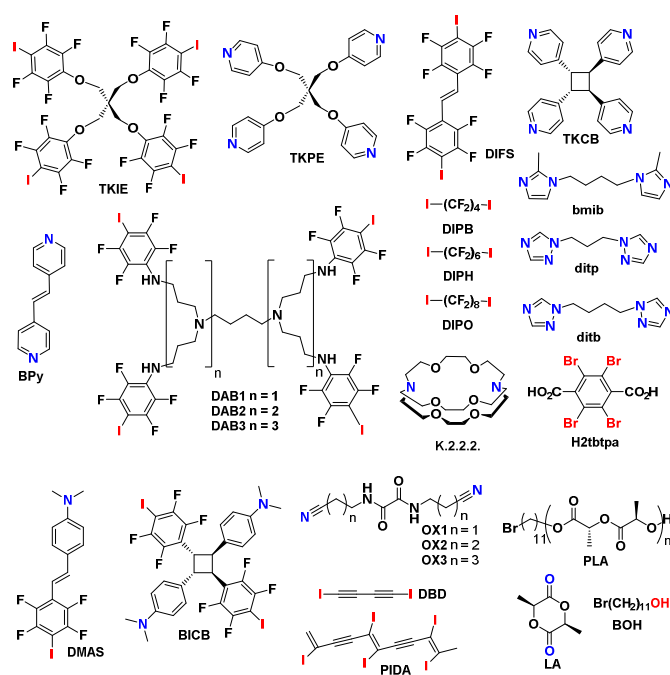
Figure 12. Structures of compounds involved in interpenetrated networks and synthetic chemistry.

As aforementioned, the applications of halogen bonds in synthetic chemistry have become increasingly important. Therefore, the preparation of new and efficient chiral XB ligands is expected shortly for applications in asymmetric catalysis.[124]

Separation and inclusion methodologies

Separation methods

From a safety, environmental and economic viewpoint, separation and purification techniques have arisen as key parameters in synthetic methodologies. In 1999, Resnati and co-workers reported the self-assembly of enantiopure (-)-sparteine hydrobromide (**SH**) and racemic 1,2-dibromohexafluoropropane (**DBFP**) (**Figure 15**). The co-crystallization of both compounds in chloroform was performed under a classical procedure which gave rise to yellow materials with a melting point dramatically different from starting compounds, in agreement with a stable crystalline supramolecular complex. The X-ray structure revealed the formation of a polymeric helical structure where halogen bonds involving bromide anions of **SH** and bromide atoms of **DBFP** connected both units. The Br$\cdots$Br$^-$ distance is quick short (3.3 Å) which represents a reduction of about 20% of the sum of the van der Waals radii. By focusing on the perfluorocarbon unit, it can be observed that only the (*S*)-enantiomer composed the polymeric complex. Thus, this methodology afforded a simple and efficient pathway for the chiral resolution of halogenoperfluorocarbon racemates.[125]

Later, another convenient separation technique based on molecular imprinting was elaborated. In general, the procedure consists in the copolymerization of a functional monomer, a cross-linker and a template. Monomers interact with the template while the cross-linkers lock the orientation of functional groups.[126] Taking into consideration the requirement for such imprinted polymers, the selective recognition toward 4-dimethylaminopyridine (**DMAP**) was envisioned through the construction of a functional macromolecule possessing 2,3,5,6-tetrafluoro-4-iodostyrene (**TFIS**) units as halogen bond donors, with divinylbenzene and styrene as crosslinkers (**Figure 15**). The polymerization reaction was run in chloroform in the presence of 2,2'-azobis(2,4-dimethyl valeronitrile) as radical initiator for 12h. Then, the template removal from polymer was carried out with methanol, followed by the evaluation of the binding and imprint properties of the resulting material. Purposely, the selectivity was measured by a competitive experiment where **DMAP** was challenged with selected substrates bearing an amino (*N,N*-dimethylamino) or a pyridyl function. Taking advantage of the presence of two electron donor sites for N$\cdots$I interactions, **DMAP** endowed a very high affinity for the porous polymer, higher than that of other compounds excepting 4-aminopyridine. Indeed, the steric hindrance appeared to affect the recognition process and consequently, the less bulky 4-aminopyridine showed a selectivity 1.7 times higher than **DMAP** for the cavities.[127]

The separation of α,ω-diiodoperfluoroalkanes (**DIPFA$_m$**) mixtures was proposed in a selective and reversible manner by means of bis(trimethylammonium) alkane diiodides (**BTAA$_{m+6}$**) according to I$\cdots$I$^-$ halogen bonding (**Figure 15**). In general, halide anions behave as good electron donors toward haloperfluoroalkanes. In this case, the crystallization process

demonstrated a good size matching between **BTAA$_{m+6}$** and **DIPFA$_m$** which allowed a further separation step. According to the crystal structures of **BTAA$_{m+6}$** and **DIPFA$_m$** partners, N$^+$-N$^+$ intramolecular distances matched well with the I$^-$-I$^-$ separations observed in the I$^-\cdots$I(CF$_2$)$_n$I$\cdots$I$^-$ superanions, the distances being in the range 0.69-0.85 Å. In addition, the 2D polymeric systems showed a similar crystal packing whereas mismatched complexes crystallized with a different supramolecular organization and stoichiometry, as well. Studies have subsequently consisted in competitive experiments. Purposely, a methanol solution of one equivalent of a single salt **BTAA$_{m+6}$** was mixed to a chloroform solution of one equivalent of each **DIPFA$_m$**. In all cases, the recognition process has conducted to the sole crystallization of size-matched complexes **BTAA$_{m+6}$** and **DIPFA$_m$**. In practice, this procedure was extended successfully to the separation of longer α,ω-diiodoperfluoroalkanes obtained from distillation residues. In a second step, the reversible character of the procedure was determined by vapor phase experiments. After crystallization of matched pairs **BTAA$_{m+6}$** and **DIPFA$_m$**, a thermal treatment afforded a complete release of iodo derivatives, as determined by TGA. Interestingly, when exposed to vapors of matching **DIPFA$_m$**, the resulting nonporous salts **BTAA$_{m+6}$** underwent a gas solid reaction with the encapsulation of host perfluorocarbons in a 1:1 ratio. ~~Finally,~~ Under exposure of a mismatched complex to vapors of matching **DIPFA$_m$**, the mismatched fluorinated compound was substituted for matching **DIPFA$_m$** owing to a similar gas solid transformation. Hence, the selective catch and release provided a simple and appealing methodology for the purification and recycling of organic components.[128] Finally, in the field of separation and recycling procedures, it is worth mentioning a simple halogen bonded recyclable catalyst used in the frame of the Morita–Baylis–Hillman reaction.[129]

Inclusion methods

In 2008, the controlled design of (6,3) honeycomb networks was proposed by the self-assembly of a three component system. It was reasoned that 1,3,5-trifluoro-2,4,6-triiodobenzene (**TFTIB**) and iodide salts could interact in order to provide halogen bonded networks due to I$\cdots$I$^-$ connections. In order to control the formation of hexagonal patterns, a mutual induced fitting process was expected between trigonal **TFTIB** and spherical anions (with potential multidentate binding) by the accommodation of a selected cation moiety of the right size. A set of ammonium, phosphonium and sulfonium iodides with different cation sizes were evaluated in recognition processes with **TFTIB** as halogen bond donor (**Figure 15**). As a result, frameworks with (6,3) topologies were obtained when trimethyl sulphonium iodide, tetraethyl and *n*-propyl ammonium iodides and tetraethyl phosphonium iodide were employed. The 2D supramolecular architectures were supported by I$\cdots$I$^-$ contacts where the small cationic entities occupied the center of the hexagonal patterns. Interestingly, on increasing the cation size, the anionic polymeric layers changed from perfectly planar to wavy 2D layers on going from small

sulfonium to phosphonium cations. When bulkier tetra-*n*-butyl ammonium and tetraphenyl phosphonium cations were assessed, the supramolecular anionic scaffolds developed totally different networks. The almost isostructural hexagonal shapes of systems $Et_4N^+I^-$/**TFTIB** and $Et_4P^+I^-$/**TFTIB** afforded to highlight the role of structure directing agent of cations in the construction of (6,3) networks. According to competitive experiments involving **TFTIB**, $Et_4N^+I^-$ and $Et_4P^+I^-$ in 1/0.5/0.5, 1.0/0.3/0.7, and 1.0/0.7/0.3 molar ratios, the resulting crystalline patterns appeared isostructural with complexes $Et_4N^+I^-$/**TFTIB** and $Et_4P^+I^-$/**TFTIB**, and the molar ratios of $Et_4N^+I^-$ and $Et_4P^+I^-$ cations in the crystals matched well with initial concentrations.[130] It can be added that the deliberate formation of (6.3) honeycomb networks was also investigated with organic salts and 1,3,5-tris(iodoethynyl)-2,4,6-trifluorobenzene (**TITF**) as tritopic halogen bond donor (see the interpenetrated networks section).[109]
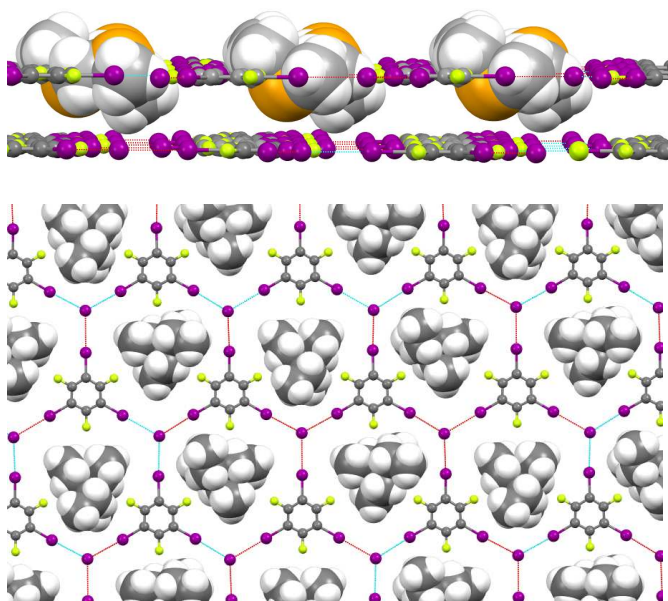
Figure 13. X-ray structure of complex trimethyl sulphonium iodide/**TFTIB** showing the perfect planarity of anionic layers with accommodated sulphonium cations in the upper layer (up). X-ray structure of complex $Et_4N^+I^-$/**TFTIB** highlighting the perfect size matching of ammonium cations in the hexagonal anionic lattice (down). Colors are as follow: C, grey; H, white; S, orange; N, blue; I, purple; F, yellow.

At the same time, the trigonal 1,3,5-tris(4-iodophenoxycarbonyl) benzene (**TIB**) was designed in order to form crystalline inclusion complexes (**Figure 15**). The crystallization of **TIB** from chloroform disclosed 2D supramolecular networks governed by C=O···I and π···I interactions. The triangular motifs formed 2D hexagonal patterns arranged in a parallel fashion. Chloroform molecules accommodated in the center of the honeycomb-like structure developing nanometer-sized channels of 1.3 nm, the porosity of the system was found to be 37.9%. Under a similar procedure, the evaporation of a pyridine solution of **TIB** gave rise to an identical arrangement with clathrated pyridine molecules.

Surprisingly, **TIB** units were exclusively connected by C=O···I and π···I contacts, no N···I halogen bond was observed in the 2D polymeric system.[131]

The accommodation of solvent molecules was also considered by the self-assembly of hexamethylenetetramine (HMTA) and *N*-iodosuccinimide (NIS). Thus, crystallographic data of [HMTA]•[NIS]$_4$ complexes demonstrated very short N···I halogen bonds with a guest molecule acting as template. A breathing behavior was highlighted owing to a thin modulation of the channel structures as a function of solvent guests. It was also demonstrated the opportunity to realize a single-crystal to single-crystal solvent exchange in solution and gas phases from a preformed system.[132,133]

Magnetic and conducting organic materials

In the 1990's, several research groups have successfully applied the halogen bonds to the field of molecular conductors. Indeed, the construction of crystalline organic metals relies on the oxidation of tetrathiafulvalene (TTF) derivatives and their association by anion coordination.[134,135] In 1995, Kato and co-workers evaluated the halogen bonds as counterpart of the hydrogen bonds. Indeed, the strength and directionality of XB was found suitable for the organization of unsymmetrical TTF derivatives. Iodination of **EDT-TTF** with ICl provided the corresponding mono and diiodo derivatives **IEDT** and **DIET** which were separated by chromatography (**Figure 15**). Then, radical cation salts were prepared by galvanostatic oxidation with various counter anions, among which $Ag(CN)_2$ and Br species. The X-ray arrangements of **IEDT**/$Ag(CN)_2$ and **IEDT**/Br were governed by I···N and I···Br$^-$ halogen bonds, each anion binding two **IEDT**. However, the structural organizations were dependent of the anion shape since **IEDT**/$Ag(CN)_2$ adopted step-like structures while **IEDT**/Br remained on the same planar level. As concerns their physical properties, all salts derived from **IEDT** and **DIET** were almost semiconductive from room temperature with small activation energies.[136] In the same trend, the structural organization of molecular conductors was engineered using halogen bond donors as neutral molecule sheathing. The non-covalent bond was supposed to create supramolecular insulating networks in order to spatially divide and confine the conducting compounds into nanowires. In this regard, six conducting compounds (**EDT-TTF, EDST, MDT-TTF, HMTSF, PT** and **TSF**) were crystallized in the presence of neutral iodo derivatives (**TIE**, **DFBIB** and **HFTIEB**) and anions as electron donors (**Figure 15**). The high strength and directionality of the I···X$^-$ (X = Cl, Br, I) halogen bonds allowed for the formation of 3D supramolecular arrangements (**Figure 14**). Thus, corresponding halogen bonded complexes (**EDT-TTF**)$_4$**BrI**$_2$(**TIE**)$_5$, (**EDST**)$_4$**I**$_3$(**TIE**)$_5$, (**MDT-TTF**)$_4$**BrI**$_2$(**TIE**)$_5$, (**HMTSF**)$_2$**Cl**$_2$(**TIE**)$_3$ and (**TSF**)**Cl**(**HFTIEB**) featured a 1D columnar organization of stacked donor radical cations and **PT** developed twisted face-to-face pairs in (**PT**)$_2$**Cl**(**DFBIB**)$_2$. Anions showed varied coordination numbers in the range 2 to 8, forming square, pentagonal and hexagonal 1D channels.

Afterwards, the physical properties of crystalline materials were evaluated by resistivity and anisotropy measurements. The best performance was achieved by **(TSF)Cl(HFTIEB)** which consisted in a supramolecular sheath of 1 nm thickness. At room temperature, the compound demonstrated a conduction anisotropy of 10^8 (resistivities were 1×10^{13}, 5×10^5 and 1×10^5 Ω cm along the a, b and c directions, respectively) which is one of the highest values reported to date for single chemical component.[137]
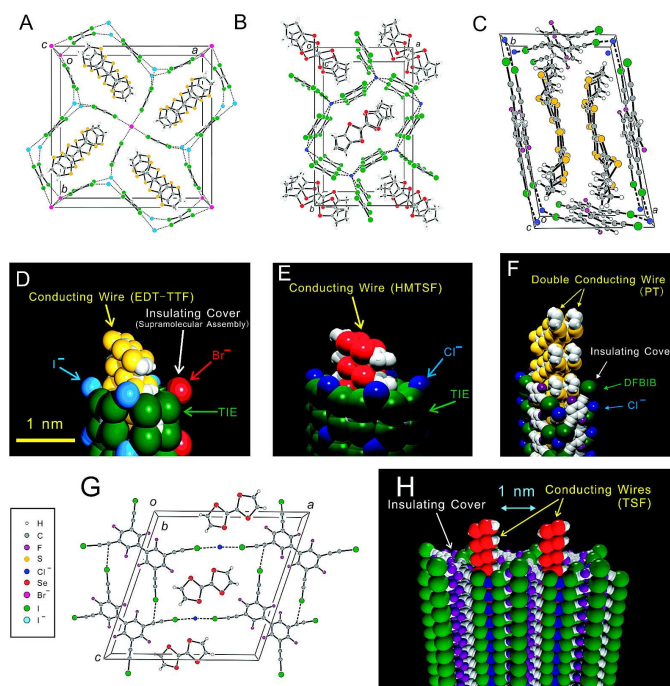
Figure 14. Crystal structures for **(EDT-TTF)₄BrI₂(TIE)₅** (A), **(HMTSF)₂Cl₂(TIE)₃** (B), **(PT)₂Cl(DFBIB)₂** (C), and **(TSF)Cl(HFTIEB)** (G). The dotted lines denote the "halogen bond" based on Lewis acidity of the neutral iodine atoms. The nanowire structures constructed in **(EDT-TTF)₄BrI₂(TIE)₅** (D), **(HMTSF)₂Cl₂(TIE)₃** (E), **(PT)₂Cl(DFBIB)₂** (F), and **(TSF)Cl(HFTIEB)** (H) are also presented in CPK modeling. White, gray, purple, yellow, blue, red, magenta, green, and sky blue denote hydrogen, carbon, fluorine, sulfur, chloride ion, selenium, bromide ion, iodine, and iodide ion in panels A–H (Reproduced from Ref. [137] with permission from the American Chemical Society).

Following the same principle, an original architecture was obtained through conducting material formation using **PT** and the halogen bond donor **PDB** in the presence of PPh₄Cl or PPh₄Br (**Figure 15**). Electrocrystallization experiments provided isostructural structures for **PT/PDB/Cl** and **PT/PDB/Br** with a 1:1:1 stoichiometry. Each anion was connected to four iodine of four different **PDB** which formed square patterns. From the geometrical point of view, the long side groups of **PDB** induced the creation of an 8-fold interpenetrated network of class Ia with a PtS topology. The fully oxidized PT•⁺ moieties were organized in 2D Heisenberg tetragonal lattices with an insulating behavior and very weak antiferromagnetic interactions.[138] It is noteworthy that other recent works have investigated the formation of halogen bonded conductive and magnetic materials involving chiral compounds.[139,140]
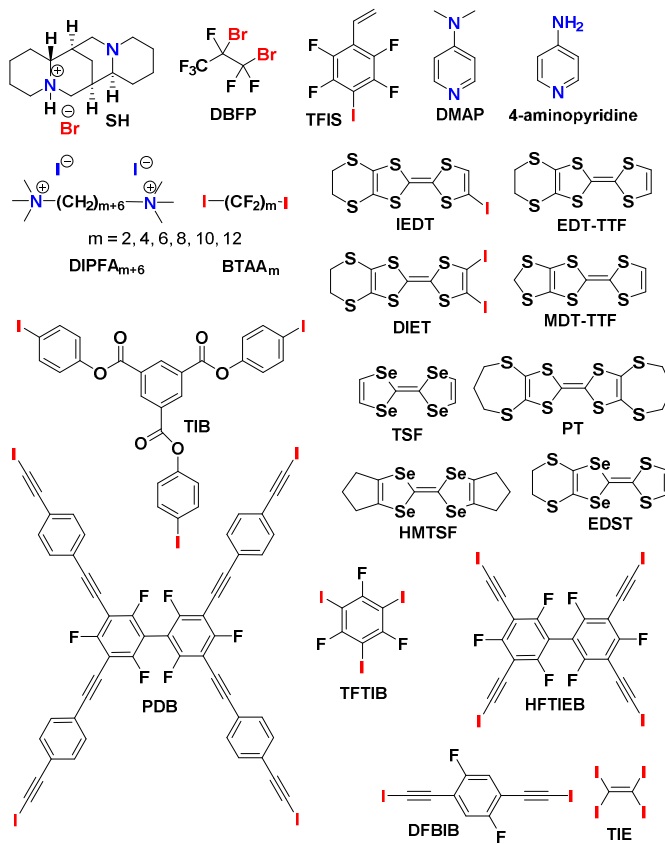
Figure 15. Structures of compounds involved in separation and inclusion methods and magnetic materials.

In order to conclude this section, it can be added that polymer-based solar cells are typically processed from solution in organic solvents. Since the morphology of the photoactive layer has a great influence on the photovoltaic device performances, the relative organization of polymeric chains through halogen bonds could bring a new insight for the construction of organic photovoltaic cells.

Conclusions

In many aspects, the field of halogen bonding (XB) has emerged as a new paradigm in materials science, biological systems and synthetic chemistry. Thus, the main features of XB account for a high directionality competing successfully with the hydrogen bonds and a tunable strength of interaction as a function of the nearest environment of halogen atoms. In the same way, its particular intrinsic hydrophobicity arises as a strong advantage over the hydrogen bonds for recognition processes operating in aqueous media and biological entities. Actually, a wide array of analytical techniques, including spectroscopic and X-ray diffraction methodologies, allow for the determination of effective XB interactions in

supramolecular complexes, and further developments are expected to expand the scope of potential applications.

The deliberate construction of halogen bonded materials is actually attracting a steady interest, relying on the inspiration of hydrogen bonded models and the intrinsic properties commented above. Here, we reported some success stories in the field of halogen bonded mono-, bi- and three-dimensional polymeric systems. The surface functionalization is highly desirable to tailor the chemical and physical behavior of substrates in a reliable fashion. Hence, polymeric materials were organized on flat substrates with a high precision owing to the strength and directionality of XB. This approach was subsequently extended to functionalized nanoparticles while (self-)complementary molecular entities gave rise to thin supramolecular architectures at the nanometer scale. Based on purpose-built components, self-assembly processes commanded by XB offered an accurate strategy to elaborate complicated entangled systems whose applications have shifted from crystal engineering to semiconducting materials. Moreover, the rational design of molecular structures provided an elegant and efficient approach for the selective separation, accommodation and confinement of compounds. Aside from these considerations, the bottom-up fabrication represents a key concept for nanotechnologies. Accordingly, the halogen bonds were able to form liquid crystalline polymers from non-mesogenic starting compounds and to induce gelation in cooperation with hydrogen bonds. Following the same bottom-up principle, luminescent materials were achieved by taking advantage of intrinsic properties of a heavy atom capable of connecting the elemental constituents into smart systems. Finally, the development of halogen bonded catalysts is slowly emerging in the frame of environmentally friendlier production, including, here, exquisite methodologies for polymer syntheses.

As far as perspectives are concerned, the occurrence and the role of XB in biological systems was recently in the limelight through *a posteriori* analyses of the Protein Data Bank, but the prominent source of halogen-containing structures holds great promise for similar discoveries, in light of these recent findings. Other striking developments are expected to come out owing to the fast growing notoriety of halogen bonding in crystal engineering and materials science. Finally, in a near future, more complicated systems are supposed to be engineered in a way to combine cooperative or competitive interactions.

Acknowledgments

Conflicts of Interest

"The authors declare no conflict of interest".

Notes and references

a Chimie Pharmaceutique Organique, Faculty of Pharmacy, Université Libre de Bruxelles (ULB), Boulevard du Triomphe, 1050 Bruxelles, Belgium.

b Laboratory of Biopolymers and Supramolecular Nanomaterials, Faculty of Pharmacy, Université Libre de Bruxelles (ULB), Campus de la Plaine, Boulevard du Triomphe, 1050 Bruxelles, Belgium.
E-mail: franck.meyer@ulb.ac.be

1 P. A. Gale and J. W. Steed. *Supramolecular Chemistry: from molecules to nanomaterials*. 1st ed. New York: John Wiley & Sons Ltd; 2012.

2 J. M. Lehn, *Proc. Natl. Acad. Sci. USA* 2002, **99**, 4763.

3 A. V. Jentzsch, A. Hennig, J. Mareda and S. Matile, *Acc. Chem. Res.* 2013, **46**, 2791.

4 M. Egli and S. Sarkhel, *Acc. Chem. Res.* 2007, **40**, 197.

5 P. Metrangolo and G. Resnati. *Halogen Bonding: Fundamentals and Applications (Structure and Bonding)*, Springer: Heidelberg, 2010.

6 F. Guthrie, *J. Chem. Soc.* 1963, **16**, 239.

7 O. Hassel, *Science* 1970, **170**, 497.

8 E. Corradi, S. V. Meille, M. T. Messina, P. Metrangolo and G. Resnati, *Angew. Chem. Int. Ed.* 2000, **39**, 1782.

9 P. Metrangolo, H. Neukirch, T. Pilati and G. Resnati, *Acc. Chem. Res.*, 2005, **38**, 386.

10 P. Metrangolo, F. Meyer, T. Pilati, G. Resnati and G. Terraneo, *Angew. Chem. Int. Ed. Engl.* 2008, **47**, 6114.

11 T. Clark, M. Hennemann, J. S. Murray and P. Politzer, *J. Mol. Model.* 2007, **13**, 291.

12 L. P. Wolters, P. Schyman, M. J. Pavan, W. L. Jorgensen, F. M. Bickelhaupt and S. Kozuch, *WIREs Comput. Mol. Sci.* 2014, **4**, 523.

13 L. Brammer, E. A. Bruton and P. Sherwood, *Cryst. Growth Des.* 2001, **1**, 277.

14 C. B. Aakeröy, M. Fasulo, N. Schultheiss, J. Desper and C. Moore, *J. Am. Chem. Soc.* 2007, **129**, 13772.

15 K. E. Riley, J. S. Murray, J. Fanfrlík, J. Rezáč, R. J. Solá, M. C. Concha, F. M. Ramos and P. Politzer, *J. Mol. Model.* 2011, **17**, 3309.

16 K. Rissanen, *CrystEngComm*, 2008, **10**, 1107.

17 C. B. Aakeröy and C. L. Spartz, *Top Curr. Chem.* 2015, **358**, 155.

18 F. Meyer and P. Dubois, *CrystEngComm* 2013, **15**, 3058.

19 A. Priimagi, G. Cavallo, P. Metrangolo and G. Resnati, *Acc. Chem. Res.* 2013, **46**, 2686.

20 P. Auffinger, F. A. Hays, E. Westhof and P. S. Ho, *Proc. Nat. Acad. Sci. USA* 2004, **101**, 16789.

21 E. Parisini, P. Metrangolo, T. Pilati, G. Resnati and G. Terraneo, *Chem. Soc. Rev.* 2011, **40**, 2267.

22 R. Wilcken, X. Liu, M. O. Zimmermann, T. J. Rutherford, A. R. Fersht, A. C. Joerger and F. M. Boeckler, *J. Am. Chem. Soc.* 2012, **134**, 6810.

23 A. V. Jentzsch and S. Matile, *Top Curr. Chem.* 2015, **358**, 205.

24 R. Wilcken, M. O. Zimmermann, A. Lange, A. C. Joerger and F. M. Boeckler, *J. Med. Chem.* 2013, **56**, 1363

25 P. S. Ho, *Top Curr. Chem.* 2015, **358**, 241.

26 A. Abate, S. Biella, G. Cavallo, F. Meyer, H. Neukirch, P. Metrangolo, T. Pilati, G. Resnati and G. Terraneo, *J. Fluor. Chem.* 2009, **130**, 1171.

27 R. Berger, G. Resnati, P. Metrangolo, E. Weber and J. Hulliger, *Chem. Soc. Rev.* 2011, **40**, 3496.

28 S. B. Poly, B. R. Bertani, P. Metrangolo, A. Moiana, E. Perez, T. Pilati, G. Resnati, I. Rico-lattes and A. Sassi, *Adv. Mater.* 2002, **14**, 1197.

29 J. Borges and J. F. Mano, *Chem. Rev.* 2014, **114**, 8883.

30 F. Wang, N. Ma, Q. Chen, W. Wang and L. Wang, *Langmuir* 2007, **23**, 9540.

31 E. Cariati, A. Forni, S. Biella, P. Metrangolo, F. Meyer, G. Resnati, S. Righetto, E. Tordin and R. Ugo, *Chem. Commun.* 2007, 2590.

32 E. Cariati, G. Cavallo, A. Forni, G. Leem, P. Metrangolo, F. Meyer, T. Pilati, G. Resnati, S. Righetto, G. Terraneo and E. Tordin, *Cryst. Growth Des.* 2011, **11**, 5642.

33 T. Shirman, D. Freeman, Y. D. Posner, I. Feldman, A. Facchetti and M. E. van der Boom, *J. Am. Chem. Soc.* 2008, **130**, 8162.

34 S. Clément, F. Meyer, J. De Winter, O. Coulembier, C. M. L. Vande Velde, M. Zeller, P. Gerbaux, J.-Y. Balandier, S. Sergeyev, R. Lazzaroni, Y. Geerts and P. Dubois, *J. Org. Chem.* 2010, **75**, 1561.

35 A. Bocheux, I. Tahar-Djebbar, C. Fiorini-Debuisschert, L. Douillard, F. Mathevet, A.-J. Attias and F. Charra, *Langmuir* 2011, **27**, 10251.

36 R. B. Wehrspohn. *Ordered Porous Nanostructures and Applications*. 1th ed. New York: Springer; **2005**.

37 G. Berger, J. Soubhye, A. van der Lee, C. Vande Velde, R. Wintjens, P. Dubois, S. Clément and F. Meyer, *ChemPlusChem* 2014, **79**, 552.

38 K.-H. Chung, J. Park, K. Y. Kim, J. K. Yoon, H. Kim, S. Han and S.-J. Kahng, *Chem. Commun.* 2011, **47**, 11492.

39 Y.-L. Zhao and J. F. Stoddart, *Acc. Chem. Res.* 2009, **42**, 1161.

40 F. Meyer, J.-M. Raquez, O. Coulembier, J. De Winter, P. Gerbaux and P. Dubois, *Chem. Commun.* 2010, **46**, 5527.

41 F. Meyer, J. Raquez, P. Verge, I. Martínez de Arenaza, B. Coto, P. Van der Voort, E. Meaurio, B. Dervaux, J. Sarasua, F. Du Prez and P. Dubois, *Biomacromolecules* 2011, **12**, 4086.

42 F. Meyer, A. Minoia, J. M. Raquez, M. Spasova, R. Lazzaroni, P. Dubois, *J. Mater. Chem.* 2010, **20**, 6873.

43 H.J. Salavagione, G. Martínez and C. Marco, *J. Mater. Chem.* 2012, **22**, 7020.

44 H. J. Salavagione, G. Ellis and G. Martínez, *J. Phys. Chem. C* 2012, **116**, 18256.

45 K. Saha, S. S. Agasti, C. Kim, X. Li and V. M. Rotello, *Chem. Rev.* 2012, **112**, 2739.

46 A. Corma and H. Garcia, *Chem. Soc. Rev.* 2008, **37**, 2096.

47 L. Dykman and N. Khlebtsov, *Chem. Soc. Rev.* 2012, **41**, 2256.

48 T. Shirman, T. Arad and M. E. van der Boom, *Angew. Chem. Int. Ed. Engl.* 2010, **49,** 926.

49 T. Shirman, R. Kaminker, D. Freeman and M. E. van der Boom, *ACS Nano* 2011, **5**, 6553.

50 A. Olivier, F. Meyer, J.-M. Raquez, P. Damman and P. Dubois, *Prog. Polym. Sci.*, 2012, **37**, 157.

51 A. Olivier, F. Meyer, S. Desbief, P. Verge, J.-M. Raquez, P. Damman, R. Lazzaroni and P. Dubois, *Chem. Commun.*, 2011, **47**, 1163.

52 A. Olivier, F. Meyer, J.-M. Raquez, P. Damman and P. Dubois, *e-Polymers* 2013, 009.

53 J. Pilate, J.-M. Renoirt, C. Caucheteur, J.-M. Raquez, F. Meyer, P. Mégret, P. Dubois and P. Damman, *Polym. Chem.* 2014, **5**, 2506.

54 P. G. De Gennes and J. Prost. *The Physics of Liquid Crystals*, Clarendon, Oxford, **1995**.

55 H. L. Nguyen, P. N. Horton, M. B. Hursthouse, A. C. Legon and D. W. Bruce, *J. Am. Chem. Soc.* 2004, **126**, 16.

56 P. Metrangolo, C. Präsang, G. Resnati, R. Liantonio, A. C. Whitwood and D. W. Bruce, *Chem. Commun.* 2006, 3290.

57 J. Xu, X. Liu, J. K.-P. Ng, T. Lin and C. He, *J. Mater. Chem.* 2006, **16**, 3540.

58 D. W. Bruce, P. Metrangolo, F. Meyer, C. Präsang, G. Resnati, G. Terraneo and A. C. Whitwood, *New J. Chem.* 2008, **32**, 477.

59 D. W. Bruce, P. Metrangolo, F. Meyer, T. Pilati, C. Präsang, G. Resnati, G. Terraneo, S. G. Wainwright and A. C. Whitwood, *Chem. Eur. J.* 2010, **16**, 9511.

60 C. Präsang, H. L. Nguyen, P. N. Horton and A. C. Whitwood, D. W. Bruce, *Chem. Commun.* 2008, 6164.

61 C. Präsang, A. C. Whitwood and D. W. Bruce, *Chem. Commun.* 2008, 2137.

62 L. Gonzales, N. Gimeno, R. M. Tejedor, V. Polo, M. B. Ros, S. Uriel and J. L. Serrano, *Chem. Mater.* 2013, **25**, 4503.

63 J. Xu, X. Liu, T. Lin, J. Huang and C. He, *Macromolecules* 2005, **38,** 3554.

64 G. Cavallo, P. Metrangolo, T. Pilati, G. Resnati, M. Sansotera and G. Terraneo, *Chem. Soc. Rev.* 2010, **39**, 3772.

65 N. Houbenov, R. Milani, M. Poutanen, J. Haataja, V. Dichiarante, J. Sainio, J. Ruokolainen, G. Resnati, P. Metrangolo and O. Ikkala, *Nat. Commun.* 2014, **5**, 4043.

66 A. R. Hirst, B. Escuder, J. F. Miravet and D. K. Smith, *Angew. Chem. Int. Ed.* 2008, **47**, 8002.

67 J. A. Foster, M. O. M. Piepenbrock, G. O. Lloyd, N. Clarke, J. A. K. Howard and J. W. Steed, *Nat. Chem.* 2010, **2**, 1037.

68 L. Meazza, J. A. Foster, K. Fucke, P. Metrangolo, G. Resnati and J. W. Steed, *Nat. Chem.* 2013, **5**, 42.

69 S. Ghosh, M. K. Mishra, S. B. Kadambi, U. Ramamurty and G. R. Desiraju, *Angew. Chem. Int. Ed.* 2015, **54**, 2674.

70 A. Mukherjee and G. R. Desiraju, *IUCrJ* 2013, **1**, 49.

71 B. Aïssa, D. Therriault, E. Haddad, and W. Jamroz, *Advances in Materials Science and Engineering* 2012, Article ID 854203.

72 A. Kohler, J. S. Wilson and R. H. Friend, *Adv. Mater.* 2002, **14**, 701.

73 O. Bolton, K. Lee, H.-J. Kim, K. Y. Lin and J. Kim, *Nat. Chem.* 2011, **3**, 205.

74 O. Bolton, D. Lee, J. Jung and J. Kim, *Chem. Mater.* 2014, **26**, 6644.

75 D. Lee, O. Bolton, B. C. Kim, J. H. Youk, S. Takayama and J. Kim, *J. Am. Chem. Soc.* 2013, **135,** 6325.

76 M. S. Kwon, D. Lee, S. Seo, J. Jung and J. Kim, *Angew. Chem. Int. Ed. Engl.* 2014, **53**, 11177.

77 H. Wang, R. X. Hu, X. Pang, H. Y. Gao and W. J. Jin, *CrystEngComm* 2014, **16**, 7942.

78 S. K. Maity, S. Bera, A. Paikar, A. Pramanik and D. Haldar, *Chem. Commun.* 2013, **49**, 9051.

79 Q. Zhu, Y. J. Gao, H. Y. Gao and W. J. Jin, *J. Photochem. Photobiol. A Chem.* 2014, **289**, 31.

80 D. Yan, A. Delori, G. O. Lloyd, T. Friščić, G. M. Day, W. Jones, J. Lu, M. Wei, D. G. Evans and X. Duan, *Angew. Chem. Int. Ed. Engl.* 2011, **50**, 12483.

81 S.-Q. Zang, Y.-J. Fan, J.-B. Li, H.-W. Hou and T. C. W. Mak, *Cryst. Growth Des.* 2011, **11**, 3395.

82 M. Saccone, G. Terraneo, T. Pilati, G. Cavallo, A. Priimagi, P. Metrangolo and G. Resnati, *Acta Crystallogr. B. Struct. Sci. Cryst. Eng. Mater.* 2014, **70**, 149.

83 M. Saccone, G. Cavallo, P. Metrangolo, G. Resnati and A. Priimagi, *Top. Curr. Chem.*, 2015, DOI 10.1007/128_2014_615.

84 A. Priimagi, G. Cavallo, A. Forni, M. Gorynsztejn-Leben, M. Kaivola, P. Metrangolo, R. Milani, A. Shishido, T. Pilati, G. Resnati and G. Terraneo, *Adv. Funct. Mater.* 2012, **22**, 2572.

85 A. Priimagi, M. Saccone, G. Cavallo, A. Shishido, T. Pilati, P. Metrangolo and G. Resnati, *Adv. Mater.* 2012, **24**, OP345.

86 O. S. Bushuyev, T. C. Corkery, C. J. Barrett and T. Friščić, *Chem. Sci.* 2014, **5**, 3158.

87 M. Saccone, V. Dichiarante, A. Forni, A. Goulet-Hanssens, G. Cavallo, J. Vapaavuori, G. Terraneo, C. J. Barrett, G. Resnati, P. Metrangolo and A. Priimagi, *J. Mater. Chem. C* 2015, **3**, 759.

88 O. S. Bushuyev, A. Tomberg, T. Friščić and C. J. Barrett, *J. Am. Chem. Soc.* 2013, **135**, 12556.

89 R. S. Forgan, J.-P. Sauvage and J. F. Stoddart, *Chem. Rev.* 2011, **111**, 5434.

90 L. Carlucci, G. Ciani and D. M. Proserpio. *Networks, Topologies, and Entanglements*. In: Braga D, Grepioni F, editors. *Making Crystals by Design Methods,Techniques and Applications*, Weinheim: Wiley-VCH; **2007**, p. 58-85.

91 N. L. Kilah, M. D. Wise, C. J. Serpell, A. L. Thompson, N. G. White, K. E. Christensen and P. D. Beer, *J. Am. Chem. Soc.*, 2010, **132**, 11893.

92 B. R. Mullaney, A. L. Thompson and P. D. Beer, *Angew. Chem. Int. Ed.*, 2014, **53**, 11458.

93 J. Y. C. Lim, M. J. Cunningham, J. J. Davis and P. D. Beer, *Dalton Trans.*, 2014, **43**, 17274.

94 A. Caballero, F. Zapata, N. G. White, P. J. Costa, V. Félix and P. D. Beer, *Angew. Chem. Int. Ed.*, 2012, **51**, 1876.

95 R. Thaimattam, C. V. K. Sharma, A. Clearfield and G. R. Desiraju, *Cryst. Growth Des.* 2001, **1**, 103.

96 V. A. Blatov, A. P. Shevchenko and D. M. Proserpio, *Cryst. Growth Des.* 2014, **14**, 3576.

97 P. Metrangolo, F. Meyer, T. Pilati, D. M. Proserpio and G. Resnati, *Chem. Eur. J.* 2007, **13**, 5765.

98 M. Baldrighi, P. Metrangolo, F. Meyer, T. Pilati, D. Proserpio, G. Resnati and G. Terraneo, *J. Fluor. Chem.* 2010, **131**, 1218.

99 C. Cavallotti, P. Metrangolo, F. Meyer, F. Recupero and G. Resnati, *J. Phys. Chem. A* 2008, **112**, 9911.

100 P. Metrangolo, F. Meyer, T. Pilati, D. M. Proserpio and G. Resnati, *Cryst. Growth Des.* 2008, **8**, 654.

101 G. T. Spence and P. D. Beer, *Acc. Chem. Res.* 2013, **46**, 571.

102 A. Mele, P. Metrangolo, H. Neukirch, T. Pilati and G. Resnati, *J. Am. Chem. Soc.* 2005, **127**, 14972.

103 A. Caballero, N. G. White and P. D. Beer, *Angew. Chem. Int. Ed. Engl.* 2011, **50**, 1845.

104 V. Amico, S. V. Meille, E. Corradi, M. T. Messina and G. Resnati, *J. Am. Chem. Soc.* 1998, **120**, 8261.

105 R. Liantonio, P. Metrangolo, T. Pilati and G. Resnati, *Cryst. Growth Des.* 2003, **3**, 355.

106 R. Liantonio, P. Metrangolo, F. Meyer, T. Pilati, W. Navarrini and G. Resnati, *Chem. Commun.* 2006, 1819.

107 R. Bertani, P. Sgarbossa, A. Venzo, F. Lelj, M. Amati, G. Resnati, T. Pilati, P. Metrangolo and G. Terraneo, *Coord. Chem. Rev.* 2010, **254**, 677.

108 Z.-H. Yan, L.-L. Han, Y.-Q. Zhao, X.-Y. Li, X.-P. Wang, L. Wang and D. Sun, *CrystEngComm* 2014, **16**, 8747.

109 J. Lieffrig, O. Jeannin and M. Fourmigué, *J. Am. Chem. Soc.* 2013, **135**, 6200.

110 A. Bruckmann and M. Pena, C. Bolm, *Synlett* 2008, 900.

111 W. He, Y.-C. Ge and C.-H. Tan, *Org. Lett.* 2014, **16**, 3244.

112 S. M. Walter, F. Kniep, E. Herdtweck and S. M. Huber, *Angew. Chem. Int. Ed. Engl.* 2011, **50**, 7187.

113 F. Kniep, S. M. Walter, E. Herdtweck and S. M. Huber, *Chem. Eur. J.* 2012, **18**, 1306.

114 S. H. Jungbauer, S. M. Walter, S. Schindler, L. Rout, F. Kniep and S. M. Huber, *Chem. Commun.* 2014, **50**, 6281.

115 Y. Takeda, D. Hisakuni, C.-H. Lin and S. Minakata, *Org. Lett.* 2015, **17**, 318.

116 G. M. J. Schmidt, *Pure Appl. Chem.* 1971, **27**, 647.

117 T. Caronna, R. Liantonio, T. a Logothetis, P. Metrangolo, T. Pilati and G. Resnati, *J. Am. Chem. Soc.* 2004, **126**, 4500.

118 G. Marras, P. Metrangolo, F. Meyer, T. Pilati, G. Resnati and A. Vij, *New J. Chem.* 2006, **30**, 1397.

119 N. S. Goroff, S. M. Curtis, J. a Webb, F. W. Fowler and J. W. Lauher, *Org. Lett.* 2005, **7**, 1891.

120 A. Sun, J. W. Lauher and N. S. Goroff, *Science* 2006, **312**, 1030.

121 M. H. Chisholm, *Pure Appl. Chem.* 2010, **82**, 1647.

122 A. P. Dove, *ACS Macro Lett.* 2012, **1**, 409.

123 O. Coulembier, F. Meyer and P. Dubois, *Polym. Chem.* 2010, **1**, 434.

124 O. Coulembier, S. Moins, V. Lemaur, R. Lazzaroni and P. Dubois, *Journal of CO$_2$ Utilization.* 2015, **10**, 7.

125 A. Farina, S. V. Meille, M. T. Messina, P. Metrangolo, G. Resnati and G. Vecchio, *Angew. Chem. Int. Ed.* 1999, **38**, 2433.

126 R. Schirhagl, *Anal. Chem.* 2014, **86**, 250.

127 T. Takeuchi, Y. Minato and H. Shinmori, *Tetrahedron Lett.* 2005, **46**, 9025.

128 P. Metrangolo, Y. Carcenac, M. Lahtinen, T. Pilati, K. Rissanen, A. V. Vij and G. Resnati, *Science* 2009, **323**, 1461.

129 S. Dordonne, B. Crousse, D. Bonnet-Delpon and J. Legros, *Chem. Commun.* 2011, **47**, 5855.

130 P. Metrangolo, F. Meyer, T. Pilati, G. Resnati and G. Terraneo, *Chem. Commun.* 2008, 1635.

131 F. C. Pigge, V. R. Vangala, P. P. Kapadia, D. C. Swenson and N. P. Rath, *Chem. Commun.* 2008, 4726.

132 K. Raatikainen and K. Rissanen, *CrystEngComm* 2011, **13**, 6972.

133 K. Raatikainen and K. Rissanen, *Chem. Sci.* 2012, **3**, 1235.

134 M. Fourmigué, *Halogen bonding in conducting or magnetic molecular materials from Structure and Bonding*. In: Mingos D M P, editors. *Structure and Bonding*, Berlin Heidelberg: Springer Verlag; **2008**, p. 181-207.

135 M. Fourmigué and P. Batail, *Chem. Rev.* 2004, **104**, 5379.

136 T. Makubo, H. Sawa and R. Kato, *Synth. Met.* 1995, **73**, 117.

137 H. M. Yamamoto, Y. Kosaka, R. Maeda, J. Yamaura, A. Nakao, T. Nakamura and R. Kato, *ACS Nano* 2008, **2**, 143.

138 J. Lieffrig, H. M. Yamamoto, T. Kusamoto, H. Cui, O. Jeannin and M. Fourmigué, *Cryst. Growth Des.* 2011, **11**, 4267.

139 N. Avarvari and J. D. Wallis, *J. Mater. Chem.* 2009, **19**, 4061.

140 K. Shin, M. Brezgunova, O. Jeannin, T. Roisnel, F. Camerel, P. Auban-senzier and M. Fourmigué, *Cryst. Growth Des.* 2011, **11**, 5337.

Polymer Chemistry Accepted Manuscript

Applications of halogen bonding are reviewed in surface functionalization, soft, luminescent and magnetic materials, interpenetrated networks, synthetic methods, separation and inclusion techniques.